

***Supporting Information:***  
**Revealing Hydrogenation Reaction  
Pathways on Naked Gold  
Nanoparticles**

Leandro Luza,<sup>[a]</sup> Camila P. Rambor,<sup>[a]</sup> Aitor Gual,<sup>[b]</sup> Jesum A. Fernandes,<sup>[b]</sup>  
Dario Eberhardt,<sup>[c]</sup> and Jairton Dupont\*<sup>[a,b]</sup>

[a] Institute of Chemistry, Universidade Federal do Rio Grande do Sul, Av.  
Bento Gonçalves, 9500, 91501-970 RS, Porto Alegre (Brazil).  
E-mail: jairton.dupont@ufrgs.br , jairton.dupont@nottingham.ac.uk

[b] GSK Carbon Neutral Laboratory for Sustainable Chemistry, University of  
Nottingham, NG7 2TU, Nottingham (UK).

[c] Physics Faculty, Pontifícia Universidade Católica do Rio Grande do Sul,  
Av. Ipiranga, 6681, Porto Alegre, (Brazil).

## Section S1.

### **Literature discussion: Catalytic Performance of AuNPs Hydrogenations.**

AuNPs have been proposed as the most suitable catalyst for application in the continuous production of fine chemical and pharmaceutical intermediates because the selectivities achieved in the hydrogenations of alkynes and 1,3-dienes to alkenes are comparable and/or superior to those achieved using benchmark Pd-based.<sup>1</sup> Tables S1, S2 and S3 display a summary of selected literature examples in the hydrogenation of 1,3-dienes (research examples are limited to butadiene hydrogenation), alkynes and  $\alpha,\beta$ -unsaturated carbonyl compounds, respectively.

A key aspect in the selective hydrogenation of 1,3-dienes and alkynes to alkenes is the absence of adsorbed products on the Au surface, *i.e.*, the desorption of the formed alkenes. This fact occurs since the adsorption of the conjugated double bonds, or triple bonds are preferred over the simple ones avoiding the competition for the same adsorption sites.<sup>2</sup> For instance, DFT simulations revealed the better adsorption of  $C\equiv C$  at the edges of AuNPs compared with  $C=C$ , whereas the selectivity is determined by the binding energy of the reactants since the barriers for hydrogenation of triple and double bonds on Au are comparable.<sup>3</sup> In contrast,  $C=C$  and  $C\equiv C$  bonds are adsorbed on Pd surface and lower selectivities have been obtained. These differences in the adsorption could be responsible for the shift of the *trans/cis* ratio of 2-butenes from 1.5–2.0 (typically Pt and other Group 8-10 transition metals) to 3.0–10 in the hydrogenation of 1,3-butadienes catalyzed by Au. This fact is explained by the kinetically favorable *trans-to-cis* isomerization during the reaction caused by the favorable *cis-to-trans* adsorption at the edges and corners of AuNPs.<sup>4,5</sup>

**Table S1.** Selected examples of the Au-catalyzed hydrogenation of 1,3-dienes.

E.	Catalyst	TOF/ min <sup>-1</sup>	Sel. Alkene/ %	Sel. 1-:2-( <i>E</i> ):2-( <i>Z</i> )- Alkene/ %	Ref.
1 <sup>[a]</sup>	Au/Al <sub>2</sub> O <sub>3</sub>	46.1	> 99	60:10:30	6
2 <sup>[a]</sup>	Au/TiO <sub>2</sub>	53.1	> 99	60:10:30	6
3 <sup>[a]</sup>	Au/ZrO <sub>2</sub>	25.1	> 99	60:10:30	4,7,8
4 <sup>[a]</sup>	Au/CeO <sub>2</sub>	28.2	> 99	—	9,10
5 <sup>[a]</sup>	Au/CNT	29.0	> 99	50:30:20	11-13
6 <sup>[a]</sup>	Au(III)-MOF	9.0	> 99	60:10:30	14
7 <sup>[a]</sup>	Au/BMI·PF <sub>6</sub> /TiO <sub>2</sub>	11.0	> 99	—	15
8 <sup>[b]</sup>	Au/BMI·PF <sub>6</sub> /PVP	—	—	—	16

<sup>[a]</sup> Hydrogenation of 1,3-butadiene; <sup>[b]</sup> Hydrogenation of 1,3-cyclooctadiene.

**Table S2.** Selected examples of the Au-catalyzed hydrogenation of alkynes.

E.	Catalyst	TOF/ min <sup>-1</sup>	Sel. Alkene/ %	Sel. <i>Z</i> -Alkene/ %	Ref.
1 <sup>[a]</sup>	Au/Al <sub>2</sub> O <sub>3</sub>	18.9	> 99	—	2
2 <sup>[a]</sup>	Au/Al <sub>2</sub> O <sub>3</sub>	8.5	> 99	—	17
2 <sup>[a]</sup>	Au/GO	6.0	> 99	—	18
3 <sup>[a]</sup>	Au/TiO <sub>2</sub>	23.6	> 99	—	1
4 <sup>[b]</sup>	Au <sub>25</sub> (SR) <sub>18</sub> /TiO <sub>2</sub>	0.016	> 99	—	19
5 <sup>[b]</sup>	Au/TiO <sub>2</sub>	0.070	> 99	>99	20
6 <sup>[b]</sup>	CeO <sub>2</sub>	0.014	95	>99	21
7 <sup>[b]</sup>	Au/BMI·PF <sub>6</sub> /PVP	—	—	—	16

<sup>[a]</sup> Hydrogenation of terminal alkynes; <sup>[b]</sup> Hydrogenation of internal alkynes.

**Table S3.** Selected examples of the Au-catalyzed hydrogenation of  $\alpha,\beta$ -unsaturated carbonyl compounds.

E.	Catalyst	TOF/ min <sup>-1</sup>	Sel./ %	Ref.
1 <sup>[a]</sup>	Au/TiO <sub>2</sub>	6.89	58 (H <sub>2</sub> -ALD); 23 (ALLYL-OH)	22-24
2 <sup>[a]</sup>	Au/ZrO <sub>2</sub>	0.60	56 (H <sub>2</sub> -ALD); 43 (ALLYL-OH)	22-24
3 <sup>[b]</sup>	Au/TiO <sub>2</sub>	0.23	68 (ALLYL-OH)	25
4 <sup>[b]</sup>	Au/Fe <sub>3</sub> O <sub>4</sub>	0.27	81 (ALLYL-OH)	26
5 <sup>[b]</sup>	Au/MCM + scCO <sub>2</sub>	—	90 (ALLYL-OH)	27,28
6 <sup>[b]</sup>	Au/SBA	0.62	96 (H <sub>2</sub> -ALD)	29
7 <sup>[b]</sup>	Au-APTS/SBA	0.03	53 (ALLYL-OH)	29
8 <sup>[c]</sup>	Au/SiO <sub>2</sub>	4.40	72 (H <sub>2</sub> -ALD)	30,31
9 <sup>[c]</sup>	Au-PVA/SiO <sub>2</sub>	10.3	95 (H <sub>2</sub> -ALD)	32
10 <sup>[c]</sup>	Au/CNT	2.10	91 (H <sub>2</sub> -ALD)	11
11 <sup>[c]</sup>	Au/XC-72	0.92	63 (H <sub>2</sub> -ALD)	33
12 <sup>[c]</sup>	Au/Al <sub>2</sub> O <sub>3</sub>	7.20	78 (ALLYL-OH)	34
13 <sup>[c]</sup>	Au/ZnO	3.90	78 (ALLYL-OH)	35
14 <sup>[c]</sup>	Au/Fe <sub>2</sub> O <sub>3</sub>	3.90	86 (ALLYL-OH)	36,37
15 <sup>[c]</sup>	Au/ FeOOH	3.90	91 (ALLYL-OH)	36,37
16 <sup>[c]</sup>	Au/BPs	0.18	78 (ALLYL-OH)	38
17 <sup>[c]</sup>	Au/PIL	0.01	78 (ALLYL-OH)	39
18 <sup>[c]</sup>	Au/SPO	0.18	>99 (ALLYL-OH)	40,41
19 <sup>[d]</sup>	Au/PVP	0.03	>99 (ALLYL-OH)	42,43
20 <sup>[d]</sup>	Au <sub>25</sub> (SR) <sub>18</sub>	0.07	>99 (ALLYL-OH)	44
21 <sup>[d]</sup>	Au <sub>25</sub> (SR) <sub>18</sub> /Fe <sub>2</sub> O <sub>3</sub>	0.07	>99 (ALLYL-OH)	44
22 <sup>[d]</sup>	Au <sub>25</sub> (SR) <sub>18</sub> /TiO <sub>2</sub>	0.07	>99 (ALLYL-OH)	44

H<sub>2</sub>-ALD: Saturated aldehydes, and ALLYL-OH: allylic alcohol. <sup>[a]</sup> Hydrogenation of acrolein; <sup>[b]</sup> Hydrogenation of crotonaldehyde; <sup>[c]</sup> Hydrogenation of cinnamaldehyde; <sup>[d]</sup> Hydrogenation of a large scope of  $\alpha,\beta$ -unsaturated carbonyl compounds.

The selectivity in the hydrogenation of  $\alpha,\beta$ -unsaturated carbonyl compounds is also affected by the catalyst size because the stronger dependence of the C=O hydrogenation rate is observed on clusters size when compared to the C=C hydrogenation rate.<sup>34</sup> The C=O adsorption is favored over C=C adsorption on AuNPs smaller than 2.0 nm since it exhibited an

enhanced  $\pi$ -back-bonding. The distinct coordination modes of  $\alpha,\beta$ -unsaturated carbonyl compounds on Au and Pt-based catalysts are suggested to be the reason for the different selectivity.<sup>25</sup> Interestingly, when Pt is deposited on AuNPs, the activity is enhanced whereas the chemoselective is unaffected. This fact is observed because Pt sites are responsible for the dissociative activation of H<sub>2</sub> while the Au sites for the adsorption-activation of the substrate.<sup>31</sup>

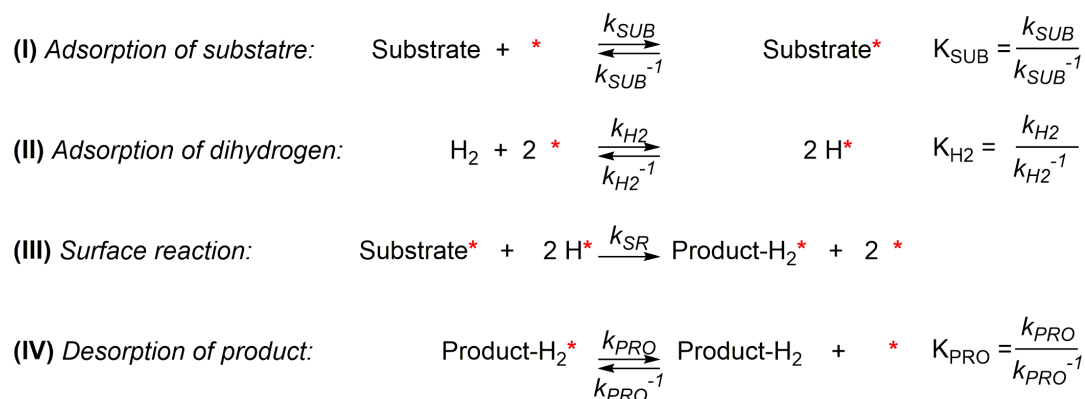
The “surface adsorption” is also the cause of the high selectivity of Au for catalyzing the epoxidation of alkenes using O<sub>2</sub>. Au-surface produced the dissociative chemisorption of O<sub>2</sub> with the advantage of not strongly perturbs the molecular structure of weakly adsorbed organic molecules and catalyzes the selective epoxidation of olefins, whereas platinum group metals produced the combustion of these compounds (carbon dioxide and water).<sup>45</sup> Furthermore, in some cases, the support can participate during the approaching of the substrate to the Au-surface. For instance, experimental and theoretical evidence reveal energetically and geometrically favored adsorption modes of substrates on TiO<sub>2</sub> and on the interface between AuNPs and TiO<sub>2</sub> support in the selective hydrogenation of  $\alpha,\beta$ -unsaturated nitro compounds by Au/TiO<sub>2</sub>.<sup>46,47</sup> Such preferential adsorption is not observed with nanoparticles of Au/SiO<sub>2</sub>.<sup>46,47</sup>

## **Section S2.**

### **Literature discussion: Mechanism and Kinetics of AuNPs Hydrogenations.**

Table S4 displays the elementary steps for the hydrogenation reaction catalyzed by metallic surfaces according to Langmuir-Hinshelwood kinetics.<sup>33,48-50</sup> Au-particles, in contrast to group 8-10 metals, exhibit unique properties, *i.e.*, the increasing capacity of H<sub>2</sub> dissociation and H<sub>2</sub> uptake as temperature increases because its dissociation over AuNPs is activated.<sup>51</sup> H<sub>2</sub> adsorption is limited by kinetic factors at moderate temperature (*ca.* between 298-373 K) and two kinetic scenarios are possible: (a) low concentration of adsorbed H because the H<sub>2</sub> dissociation is limited, and (b) H<sub>2</sub> dissociation favored and high concentration of adsorbed atomic H.<sup>48</sup>

**Table S4.** Elementary steps for hydrogenation reaction catalyzed by metallic surfaces according to Langmuir-Hinshelwood kinetics.



RDS	Model	Linearised Form
Substrate adsorption	$r = \frac{k_{\text{SUB}} \cdot [\text{SUB}]}{1 + (K_{\text{H}_2} \cdot P_{\text{H}_2})^{1/2}}$	$r^{-1} = a \cdot P_{\text{H}_2}^{1/2} + b$
Dihydrogen adsorption	$r = \frac{k_{\text{H}_2} \cdot P_{\text{H}_2}}{1 + (K_{\text{SUB}} \cdot [\text{SUB}])^2}$	$r = a \cdot P_{\text{H}_2}$
Surface reaction (competitive adsorption)	$r = \frac{k_{\text{SR}} \cdot K_{\text{SUB}} \cdot [\text{SUB}] \cdot K_{\text{H}_2} \cdot P_{\text{H}_2}}{(1 + (K_{\text{SUB}} \cdot [\text{SUB}]) + (K_{\text{H}_2} \cdot P_{\text{H}_2})^{1/2})^3}$	$(P_{\text{H}_2}/r)^{1/3} = a \cdot P_{\text{H}_2}^{1/2} + b$
Surface reaction (independent adsorption)	$r = \frac{k_{\text{SR}} \cdot K_{\text{SUB}} \cdot [\text{SUB}] \cdot K_{\text{H}_2} \cdot P_{\text{H}_2}}{(1 + (K_{\text{SUB}} \cdot [\text{SUB}])) + (1 + (K_{\text{H}_2} \cdot P_{\text{H}_2})^{1/2})^2}$	$r^{-1/2} = a \cdot P_{\text{H}_2}^{-1/2} + b$

The rate-determining step (RDS) for hydrogenations is proposed to be the dissociative adsorption of H<sub>2</sub> by the following evidence: (a) H<sub>2</sub> chemisorption, performed between 25 and 250 °C<sup>51</sup> and (b) by results of selective hydrogenation of crotonaldehyde carried out at 120 °C.<sup>25</sup> Some examples of apparent order of reaction and apparent activation energy (*E<sub>a-app</sub>*) for hydrogenations reported in the literature are: (a) for Au/Al<sub>2</sub>O<sub>3</sub> between 170 and 260 °C, *E<sub>a-app</sub>* of 36 kJ mol<sup>-1</sup> and 1 and 0 are the orders in H<sub>2</sub> and butadiene, respectively;<sup>52</sup> (b) for Au/Al<sub>2</sub>O<sub>3</sub> between 45 and 90 °C, *E<sub>a-app</sub>* of 50 kJ mol<sup>-1</sup> and 0.7 and 0 are the orders in H<sub>2</sub> and butadiene, respectively;<sup>53</sup> (c)

for Au/Al<sub>2</sub>O<sub>3</sub> between 65 and 120 °C,  $E_{a-app}$  of 34 kJ mol<sup>-1</sup> and 0.4 and 0 are the orders in H<sub>2</sub> and acetylene, respectively;<sup>54</sup> (d) for Au/SiO<sub>2</sub> between 150 and 250 °C and 1.1 and 0 are the orders in H<sub>2</sub> and acetylene, respectively;<sup>55</sup> and (e) for Au/CeO<sub>2</sub> between 50 and 300 °C 1.0 and 0 are the orders in H<sub>2</sub> and acetylene, respectively.<sup>56</sup>

The poor catalytic activity and high selectivity in the Au-catalyzed hydrogenations are well documented since a long time ago.<sup>52,57</sup> Low activities in the cyclohexene hydrogenation are owing to the low-frequency factor of catalytic active species on the Au-surface (*ca.* insufficient activation of the adsorbed olefin molecule and the concentration of adsorbed H atoms is extremely small) and not because the activation energy it is high.<sup>58</sup> This fact is due to the lack of a partially filled *d*-band at the usual temperatures and its consequent inability to chemisorb/activate simple molecules.<sup>52,57</sup>

Kinetic studies using H<sub>2</sub> and deuterium (D<sub>2</sub>) in the hydrogenation of cyclohexene to cyclohexane and the disproportionation of cyclohexene into cyclohexane and benzene catalyzed by Au-surfaces revealed interesting details about the mechanism.<sup>58</sup> The H<sub>2</sub> pressure and reaction temperature influence the course of the reaction by the control of the relative proportions of the adsorbed olefin species on the Au-surface since it was observed a minuscule quantity of H<sub>2</sub> or D<sub>2</sub> chemisorbed.<sup>58</sup> The Au-surface can catalytically activate olefins (*ca.* cyclohexene) although it has no influence on saturated hydrocarbons (*ca.* cyclohexane) and unsaturated (*ca.* benzene) is weakly chemisorbed.<sup>58</sup> The formation of cyclohexane-d<sub>0</sub> and benzene-d<sub>0</sub> suggests the occurrence of self-hydrogenation by the direct transfer of H atoms between hydrocarbon species on the catalyst surface or through chemisorbed H atoms on Au-surface (*ca.* very unlikely due to the low H concentration on Au-surfaces).<sup>59</sup> This is an important side-process during the addition of D<sub>2</sub> or chemisorbed D atoms.<sup>58</sup> Similar behavior (only H<sub>2</sub> formed and no HD) was observed in the decomposition of HCOOH in the presence of D<sub>2</sub>.<sup>60</sup>

The RDS for hydrogenations is shifted to the surface reaction by the use of additives or modifiers, which facilitate the dissociative adsorption of H<sub>2</sub>. For instance, an addition of Pt to AuNPs/SiO<sub>2</sub> shifted the concentration of the surface species, and the RDS is determined to be the surface reaction

between the independently adsorbed substrate molecules and H atoms on active sites of different nature.<sup>33</sup> Another possibility is the involvement of the ionic hydrogenation mechanism, in which H<sub>2</sub> ligands directly produce the proton transfer to the substrate with the formation of carbocations and the following hydride transfer from the metal hydride.<sup>61</sup> For organometallic complexes, there are literature examples of the ionic hydrogenation in the reduction of sterically hindered olefins<sup>62,63</sup>, ketones<sup>64,65</sup> and imines<sup>66</sup>.

### **Section S3.**

#### **Literature discussion: Hydrogen Activation and Formation of Au-hydrides in AuNPs.**

Theoretical and experimental evidence suggested that H<sub>2</sub> can be dissociated almost without additional energy by the simultaneous interaction of one low coordinated Au atom (at the edge of a NP or into an extended line defect) with the two hydrogen atoms of H<sub>2</sub>. After dissociation, the two H atoms are in bridge positions sharing the low coordinated Au-atom without inducing any significant deformation of the Au-Au distances.<sup>50,67-72</sup> The activation of H<sub>2</sub> was evaluated by carrying out the H-D exchange reaction with distinct Au/inorganic oxide (Al<sub>2</sub>O<sub>3</sub> and TiO<sub>2</sub>) support catalysts.<sup>51,57,73,74</sup> Size effect was ascribed to the higher fraction of low coordinated Au atoms present in smaller AuNPs.<sup>51,57</sup> As temperature increased two effects were observed: (a) the dissociation of H<sub>2</sub> being activated on Au and (b) increase of the rate constant for the recombination of H and D atoms.<sup>51</sup> At low temperatures (298 K), low HD:H/Au ratios are obtained, and with the increase of the temperature the recombination rate becomes faster and, thus, HD:H/Au ratios also increases.<sup>51</sup> By considering thermodynamics, the temperature effect is unexpected since for Pt group metals higher temperatures favor the H<sub>2</sub> desorption and the reduction of the H/M ratio. Interestingly, the H/Au ratio is maintained due to the kinetic factors, *i.e.*, higher temperatures facilitate the H<sub>2</sub> dissociation on AuNPs and H/Au ratio reaches the maximum at a certain temperature.<sup>51</sup> The hydrogen-Au interaction is weaker than hydrogen-Pt since: (a) to obtain the same apparent hydrogen Au coverage requires higher pressure than Pt, (b) the fraction of strongly adsorbed hydrogen is lower for

Au than for Pt particles, and (c) the H-induced effect in the XANES  $L_{3,2}$  edges is smaller for Au than for Pt.<sup>51</sup> Therefore, in contrast to the Pt group metals, the adsorption process is not in thermodynamic equilibrium and the determination of the strength of the hydrogen-Au interaction by calculating the adsorption equilibrium constants is not possible.<sup>51</sup>

The involvement of breaking/formation C-H bond and the formation of Au-H as catalytically active species in the RDS of the reaction mechanism of the following processes is proposed due to the primary kinetic isotopic effect (KIE,  $K_H/K_D$ ): (a) 1.7-2.0 for aerobic oxidation of alcohols catalyzed by Au/CeO<sub>2</sub>;<sup>75</sup> (b) 1.6 for NaBH<sub>4</sub>/NaBD<sub>4</sub> transfer hydrogenation reduction of nitroarenes catalyzed by Au/TiO<sub>2</sub>;<sup>76</sup> and (c) 1.5 for NaBH<sub>4</sub> transfer hydrogenation reduction of nitroarenes catalyzed by Au/TiO<sub>2</sub> in the presence of CO/H<sub>2</sub>O/D<sub>2</sub>O mixtures.<sup>77</sup>

Alternative H<sub>2</sub> activation pathways by the collaboration of the AuNPs with additives/support/substrate/solvent have been proposed.<sup>61</sup> This subject is presented in the below section.

## **Section S4.**

### **Literature discussion: Size Effect on Catalytic Performance of AuNPs.**

XRD pattern of the *fcc* gold lattice displays five characteristic peaks at  $2\theta = 38.1, 44.2, 64.6, 77.5,$  and  $81.4^\circ$  corresponding to the (111), (200), (220), (311), and (222) planes, respectively.<sup>78</sup> XRD pattern of the *fcc* AuNPs shows broad bands for the (111) and (200) reflections indicating that the size of the particles is in the nanometer range.<sup>79</sup> In the literature, the distribution of the atoms of the AuNPs is calculated using the truncated icosahedron model proposed by Van Hardefeld and Hartog. Using this model, the number total atoms (**N<sub>T</sub>**), number surface atoms (**N<sub>s</sub>**) and the number of atoms in planes (**A** and **B**, coordination number = 9 and 8, respectively), edges (**C** and **D**, coordination number = 7) and corners (**E**, coordination number = 6) is elucidated.<sup>80-83</sup> The reduction of the particle size conducts to the formation of particles with a lower fraction of atoms with high coordination number (planes **A** and **B**) and a higher fraction of low coordination number (edges **C** and **D**, and corner **E**).

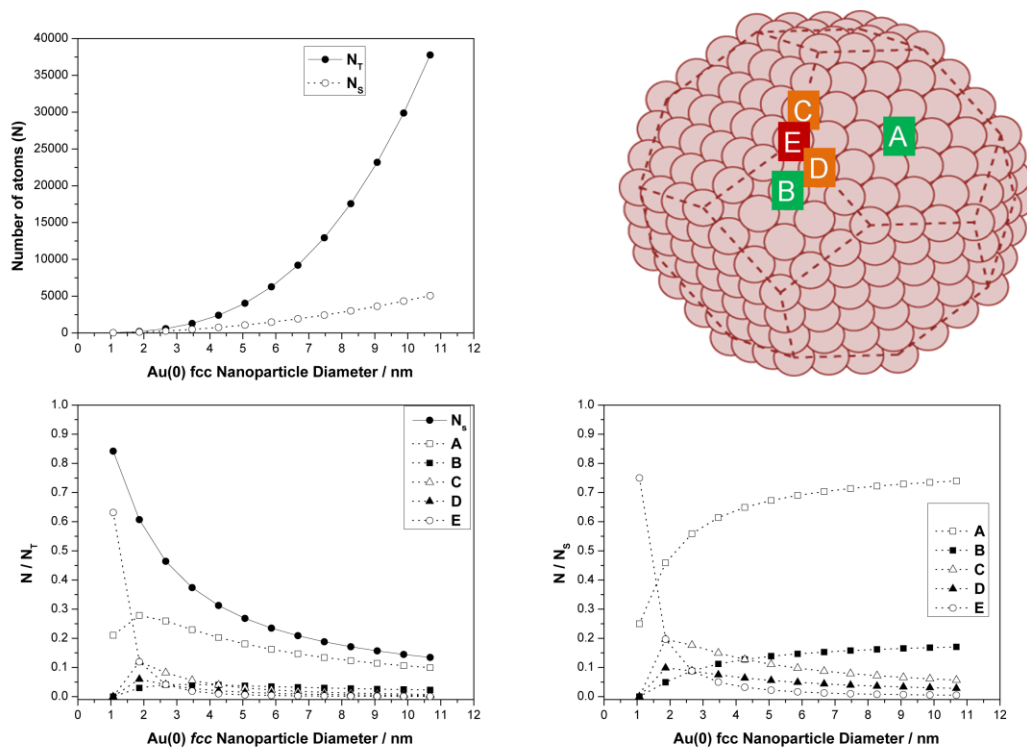


**Figure S1.** Truncated icosahedrons model of the *fcc* AuNPs suggested by Van Hardefeld and Hartog.<sup>80-83</sup>

Improvement of the hydrogenation activity and selectivity is observed by reducing the particle size to the nanometric scale.<sup>17,23-25,34,69,84</sup> This effect is explained regarding geometric and electronic factors. Smaller NPs with low coordination numbers (edges **C** and **D**, and corner **E**) and more electron deficient Au(0)-atoms facilitate the H<sub>2</sub> activation<sup>70,71</sup> and enhance the substrate/product discrimination by differences in their binding energies.<sup>45,85-87</sup> XPS studies of AuNPs show that the binding energies of the bulk Au<sup>88</sup> are shifted to higher binding energies (Au4f<sub>7/2</sub> from 83.8 to 84.3 eV) and become more positive as the AuNPs size decreases.<sup>86,89-91</sup> Therefore, size affects activity and selectivity of the AuNPs between parallel substrate/product adsorption pathways.<sup>84</sup> Thermodynamic analysis of NP size effect on reaction kinetics reveals that size variations produce many drastic changes in the selectivity of consecutive reactions than in the selectivity of parallel reactions.<sup>49</sup>

Particle sizes smaller than 2 nm are considered the most suitable because there is a combination of two factors: (a) higher fraction of low-

coordinated Au atoms<sup>92,93</sup> and (b) electronic effects caused by the nanoconfinement.<sup>94,95</sup> Other reason for the improved catalytic performance is the fact that some substrates/products (nitrobenzene) exclusively adsorbs/reacts in the low coordination sites (steps and corners) of AuNPs.<sup>86</sup> Ultrasmall Au<sub>25</sub>, Au<sub>38</sub>, Au<sub>55</sub> and Au<sub>144</sub> nanoclusters (mean diameter inferior to 1.6 nm) exhibited impressive catalytic performances due to the combination of dissociative chemisorptions of small molecules (H<sub>2</sub> and O<sub>2</sub>) necessary for triggering the subsequent catalytic chemistry and interaction with the substrate in a particular manner to attain unexpected high selectivities.<sup>19,44,96-102</sup> Smaller Au nanoclusters display larger gap between the highest occupied molecular orbital (HOMO) and lowest unoccupied molecular orbital (LUMO) (no band gap ( $E_g$ ) observed for Au<sub>144</sub> and  $E_g$  of 1.3 and 0.9 eV for Au<sub>25</sub> and Au<sub>38</sub>, respectively), and then, higher levels of non-metallic character.<sup>99</sup>

## **Section S5.**

### **Literature discussion: Support Effect on Catalytic Performance of AuNPs.**

Inorganic oxide supports are reported to affect also the electronic properties of the AuNPs and thus their catalytic properties by withdrawing (Au/Al<sub>2</sub>O<sub>3</sub>) or donating (Au/TiO<sub>2</sub>) electron density.<sup>100,103,104</sup> The support has a significant influence in the Au-reduction treatment required, and thus, in their catalytic activity. For instance, the poor activity of Au/Al<sub>2</sub>O<sub>3</sub> respect to Au/CeO<sub>2</sub> and Au/TiO<sub>2</sub> has been ascribed to the poor reducibility of the Au(III) precursor in Al<sub>2</sub>O<sub>3</sub>.<sup>105</sup> The structure of the inorganic oxides could be affected during the reduction treatment under H<sub>2</sub> atmosphere.<sup>106</sup> For instance, EPR analysis revealed the existence of electron donating paramagnetic defects (F-centers), which are trapped in an oxygen vacancy within the ZrO<sub>2</sub> support. It was also reported the reduction in hydrogen of the support atoms for reducible inorganic oxides (creation of oxygen vacancies and partial Ti(IV) reduction to Ti(III) of TiO<sub>2</sub> and Ce(IV) to Ce(III) reduction CeO<sub>2</sub>).<sup>22-24,107</sup> This reactivity of the support during the reduction treatment affects the catalytic performance. For instance, in the selective hydrogenation of  $\alpha,\beta$ -unsaturated carbonyl compounds catalyzed by Au onto distinct Fe-based supports, the

$\alpha,\beta$ -unsaturated alcohol selectivity increases with the reducibility of the support ( $\text{FeO}(\text{OH}) > \gamma\text{-Fe}_2\text{O}_3 > \alpha\text{-Fe}_2\text{O}_3$ ). This behavior is explained by the favored back-bonding to the  $\pi^*$  C=O orbital by the electron-enriched Au particles formed by electron transfers from the reduced support to the metal.<sup>36,37</sup> It was proposed that the support is non-innocent spectator during the hydrogenation reaction since it actively participates in the substrate adsorption (nitro vs. olefinic group selective hydrogenation catalyzed by Au/TiO<sub>2</sub><sup>46</sup> and *m*-nitroaniline vs. *m*-phenylenediamine selective hydrogenation catalyzed by Au onto TiO<sub>2</sub>, Fe<sub>2</sub>O<sub>3</sub>, CeO<sub>2</sub>, and Al<sub>2</sub>O<sub>3</sub><sup>103</sup>) or in the H<sub>2</sub> dissociation.<sup>108-113</sup> The ability of the support to help in the heterolytic dissociation of H<sub>2</sub> has a direct dependence on the catalyst activity and an indirect dependence with the particle size (Au/Al<sub>2</sub>O<sub>3</sub> displays higher size dependence and inferior ability to help in the H<sub>2</sub> dissociation than Au/TiO<sub>2</sub>).<sup>111,114-116</sup>

## Section S6.

### **Literature discussion: Additive Effect on Catalytic Performance of AuNPs.**

The presence of chlorine (commonly from the Au-precursor, HAuCl<sub>4</sub>) was found detrimental for selective hydrogenation of butadiene.<sup>6</sup> Additives contribute in various ways for the enhancement of the catalytic performance. One way, is the increased stabilization of the Au-nanostructure provided by polymers (poly-vinyl-alcohol (PVA)<sup>32</sup> poly-vinyl-pyrrolidone (PVP)<sup>15,16</sup>), ionic liquids (ILs) (imidazolium salts)<sup>15,16,117</sup>, highly coordinating organic molecules with basic centers (S-donor<sup>19,44,96-99,101,102</sup>, N-donor<sup>9,29,118</sup>, P-donor<sup>40,41,98</sup> and NHC<sup>119,120</sup>), solvents (DMF<sup>121</sup> and THF<sup>40,41</sup>) or even substrates (N-donor such as imines, nitriles and quinolines<sup>122-124</sup>). These molecules are involved in the catalytic process by improving the selectivity by blocking active sites responsible for undesired reactions<sup>44,98,99,101,102</sup> and enhancing the catalytic activity helping in the H<sub>2</sub> dissociation by formation of Frustrated Lewis Pairs like species (AuNPs acts as Lewis Acid and the organic molecule acts as Lewis Base).<sup>40,41,122-124</sup> The use of Frustrated Lewis Pairs and their reactivity with H<sub>2</sub> is receiving an increasing interest in the recent literature since the



using isolated Au atoms was also reported.<sup>7,8,14,130</sup> Selective hydrogenation of acetylene catalyzed by Au/CeO<sub>2</sub> with a oxygen pre-treatment produced more active catalysts than the treatment in hydrogen.<sup>2</sup> Inelastic neutron scattering of AuNPs/CeO<sub>2</sub> revealed the formation/breaking of bridging hydroxyl groups by either hydrogen treatment or treatment with oxygen source (ca. carbon dioxide (CO<sub>2</sub>) or oxygen (O<sub>2</sub>)).<sup>107</sup> The exposition of the catalysts to oxygen (O<sub>2</sub>) and carbon monoxide (CO) has been demonstrated to switch the reaction selectivity between hydrogenation and epoxidation of propene over Au/TiO<sub>2</sub> catalysts.<sup>131,132</sup> The preferential oxidation (PROX) of CO with O<sub>2</sub> is a treatment to reduce the CO levels (less than 10 ppm) and purify the hydrogen catalyzed by AuNPs, and this reaction proceeds with higher activity and selectivity in the presence of sufficient surface water (H<sub>2</sub>O) because if water is absent the catalysts is forced to oxidize H<sub>2</sub> to generate the protons.<sup>133</sup>

In the selective hydrogenation of 1,3-butadiene, the effect in the catalytic performance of the treatment of the Au/ZrO<sub>2</sub> with H<sub>2</sub>O is positive (1,3-butadiene conversion is 10-fold increased for the system treated with water) and with O<sub>2</sub> is negative (drastic deactivation).<sup>4</sup> In contrast, the 1,3-butadiene conversion produced by Au/Al<sub>2</sub>O<sub>3</sub> (a catalyst with low tendency to create oxygen vacancy) was reduced in the presence of low water concentration because the competitive adsorption with the substrate to the sites neighboring hydrogen.<sup>134</sup>

## **Section S7.**

### **Results Discussion: Synthesis and Characterization of the Au-nanocatalysts.**

<sup>13</sup>C CP-MAS NMR analysis was performed to identify the characteristic signals of the immobilized ILs (Table S5 and Figure S3). The signals observed at 12, 19, 32 and 50 ppm are related to the butyl chain substituent of the imidazolium ring whereas the signals at 11, 25 and 52 ppm are assigned to the propyl chain that connects the silicon atom to the imidazolium ring. Signals at 123 and 135 ppm are ascribed to the three imidazolium carbon atoms.<sup>135</sup> The absence of any further carbon peak confirmed the presence of unreacted Si-C bonds, even under the acidic reaction conditions.

**Table S5.**  $^{13}\text{C}$  CP-MAS NMR spectra data of the Au/ $\gamma\text{-Al}_2\text{O}_3$ , Au/**B1** and Au/**B2** catalysts.

Support	$\delta$ / ppm									
	(P1)	(P2)	(P3)	(P4)	(P5)	(P6),(P7)	(P8)	(P9)	(P10)	
Au/ $\gamma\text{-Al}_2\text{O}_3$	—	—	—	—	—	—	—	—	—	—
Au/ <b>B1</b>	11.2	19.0	32.1	49.3	136.2	122.6	51.9	25.1	11.2	
Au/ <b>B2</b>	10.7	18.8	31.8	49.8	135.4	122.8	52.3	25.0	10.7	

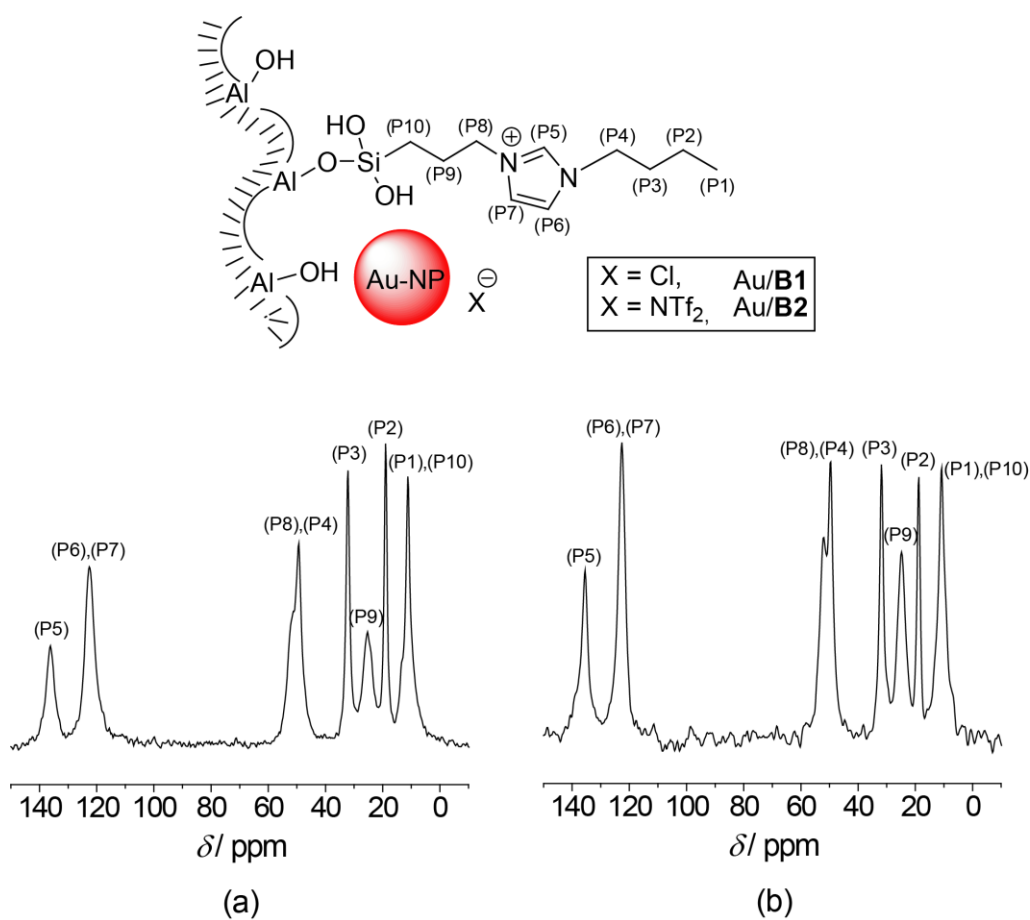


**Figure S3.**  $^{13}\text{C}$  CP-MAS NMR spectra of the a) Au/**B1** and b) Au/**B2** catalysts.

The  $^{29}\text{Si}$  CP-MAS NMR analysis is used to clarify the effect of the anion exchange step and also to estimate the IL dispersion onto surface supports. Signals at  $-46$  and  $-55$  ppm attributed to  $\text{T}^1$  ( $\text{RSi}(\text{OAl})(\text{OH})_2$ ) and  $\text{T}^2$  ( $\text{RSi}(\text{OAl})(\text{OSi})(\text{OH})$ ) species are observed for Au/**B1** and Au/**B2** catalysts with ratios of 40:60 for both cases (Table S6 and Figure S4). After  $\text{Cl}^-$

exchange, it is not observed in the catalysts Au/**B2** the appearance of the third signal at -65 ppm assigned to the T<sup>3</sup> (RSi(OAl)(OSi)<sub>2</sub>) species. These facts are of crucial importance since they suggest the presence of a homogeneous and well-dispersed IL layer onto supports, which can provide efficient stabilization for MNPs. Similar quantification of the T<sup>1</sup>, T<sup>2</sup> and T<sup>3</sup> species was carried out in the immobilization of functionalized imidazolium IL onto SiO<sub>2</sub> used for stabilization of RuNPs.<sup>136</sup>

**Table S6.** <sup>29</sup>Si CP-MAS NMR spectra data of the Au/ $\gamma$ -Al<sub>2</sub>O<sub>3</sub>, Au/**B1** and Au/**B2** catalysts.

Support	T <sup>1</sup>	T <sup>2</sup>	T <sup>3</sup>
	$\delta$ / ppm (Area/ %)	$\delta$ / ppm (Area/ %)	$\delta$ / ppm (Area/ %)
Au/ $\gamma$ -Al <sub>2</sub> O <sub>3</sub>	—	—	—
Au/ <b>B1</b>	- 46 (44)	- 55 (56)	—
Au/ <b>B2</b>	- 46 (42)	- 55 (58)	—

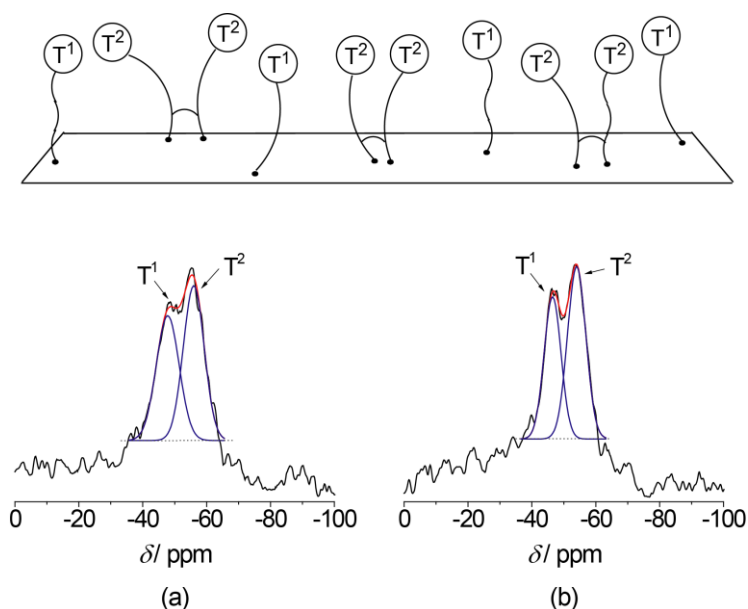


**Figure S4.** <sup>29</sup>Si CP-MAS NMR spectra of the a) Au/**B1** and b) Au/**B2** catalysts.

The FT-IR analysis of the catalysts reveal the characteristic bands of the ILs present on IL-hybrid/aluminas (Table S7 and Figure S5). The signals at 1640 and 3460  $\text{cm}^{-1}$  are assigned to the vibrations of the  $\text{H}_2\text{O}$  molecules adsorbed on catalysts. The characteristic bands about the stretching C–H of the imidazolium ring are observed at 3150  $\text{cm}^{-1}$  and to the C–H of the alkyl groups at 1465, 2880, 2940, and 2970  $\text{cm}^{-1}$ . The band at 1570  $\text{cm}^{-1}$  is the characteristic stretching frequency of the C=N and C=C bonds present in the imidazolium ring.

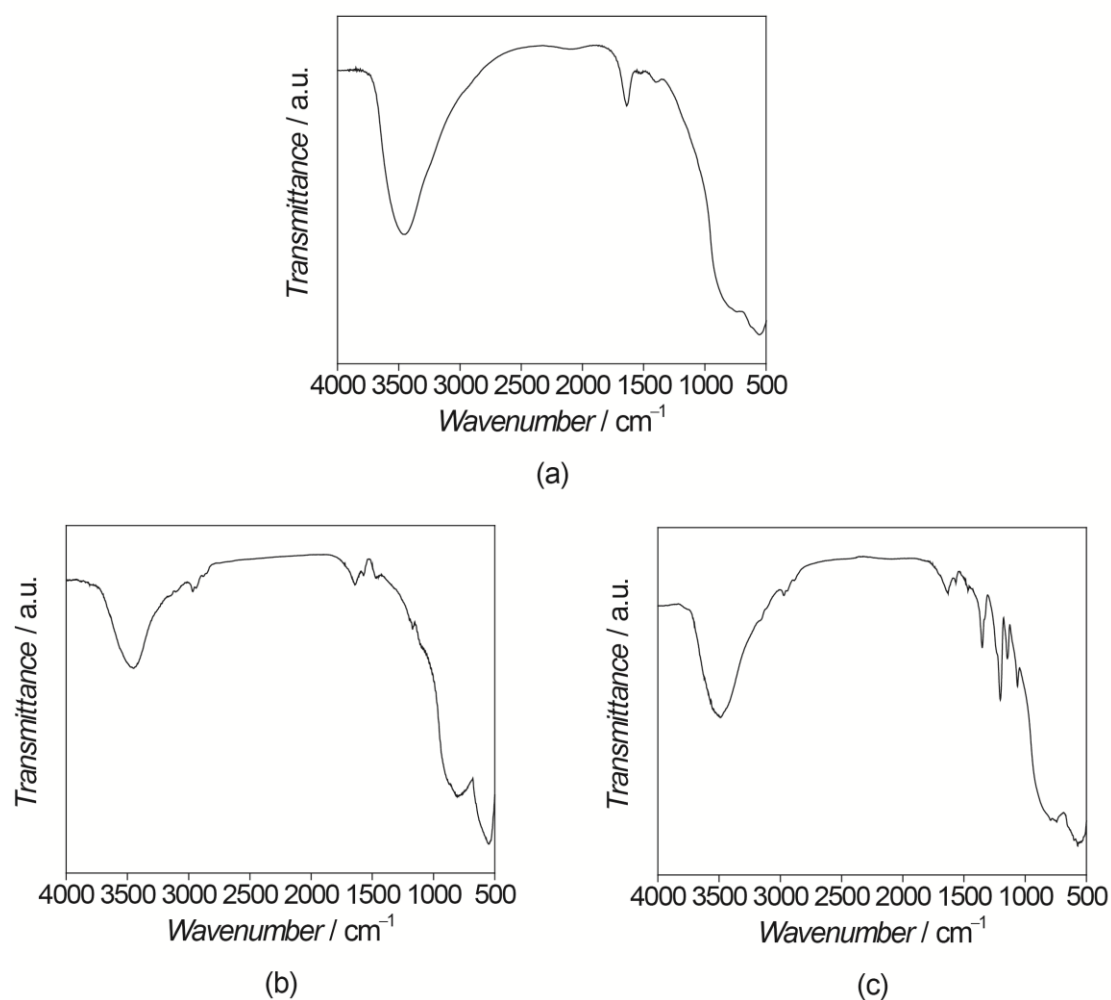


**Figure S5.** FT-IR spectra of the a) Au/ $\gamma$ - $\text{Al}_2\text{O}_3$ , b) Au/B1 and c) Au/B2 catalysts.

**Table S7.** FT-IR spectra data of the Au/ $\gamma$ -Al<sub>2</sub>O<sub>3</sub>, Au/**B1** and Au/**B2** catalysts.

Attribution	Wavenumber/ cm <sup>-1</sup>		
	Au/ $\gamma$ -Al <sub>2</sub> O <sub>3</sub>	Au/ <b>B1</b>	Au/ <b>B2</b>
$\nu$ (OH)	3460	3460	3480
$\nu$ (=C-H)	—	3150	3157
$\nu_{\text{as}}$ (C-H) <sup>a</sup>	—	2966	2970
$\nu_{\text{as}}$ (C-H) <sup>b</sup>	—	2939	2941
$\nu$ (C-H)	—	2879	2887
$\delta$ (H-O-H)	1639	1643	1636
$\nu$ (C=N)	—	1571	1566
$\nu$ (C=C)	—	1571	1566
$\delta$ (CH <sub>2</sub> )	—	1471	1467
$\nu_{\text{as}}$ (SO <sub>2</sub> )	—	—	1352
$\nu_{\text{as}}$ (SO <sub>2</sub> )	—	—	1331
$\nu_{\text{as}}$ (CF <sub>3</sub> )	—	—	1204
$\nu_{\text{as}}$ (Si-O-Si) <sub>L</sub>	—	1170	—
$\nu_{\text{as}}$ (Si-O-Si) <sub>T</sub>	—	1091	1095
$\nu$ (S-N-S)	—	—	1064

<sup>a</sup> butyl chain; <sup>b</sup> propyl chain.

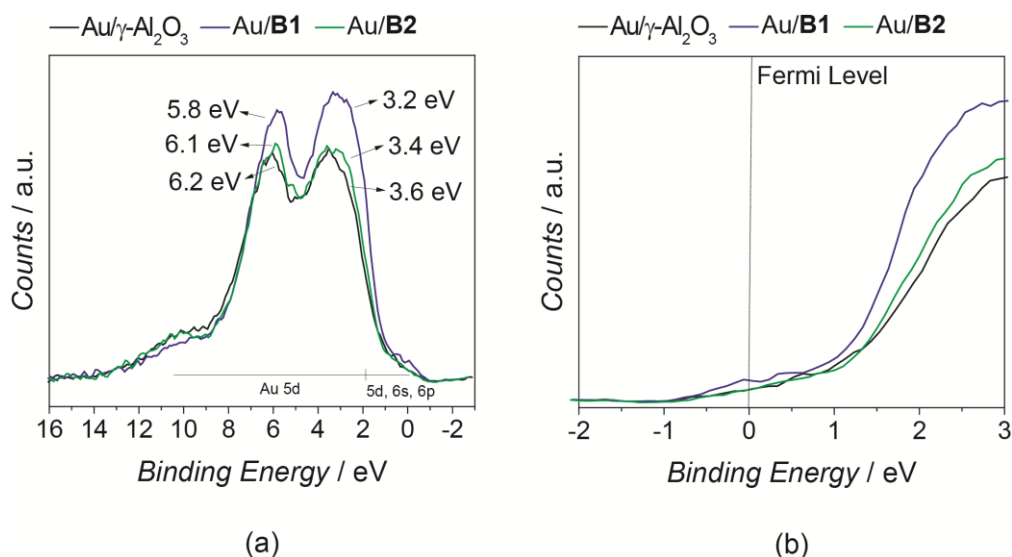


**Figure S6.** XPS measurements at Au valence band regions for the Au/γ-Al<sub>2</sub>O<sub>3</sub>, Au/B1 and Au/B2 catalysts.

**Table S8.** Composition vs. surface compositions of the Au/Al<sub>2</sub>O<sub>3</sub>, Au/B1 and Au/B2 catalysts.

E. Catalyst	IL/Au <sup>[a]</sup> (mol:mol)	Surface IL/Au <sup>[b]</sup> (mol:mol)	Al <sub>2</sub> O <sub>3</sub> /Au <sup>[a]</sup> (mol:mol)	Surface Al <sub>2</sub> O <sub>3</sub> /Au <sup>[c]</sup> (mol:mol)
1 Au/γ-Al <sub>2</sub> O <sub>3</sub>	-	-	568:1	2.8:1
2 Au/B1	22:1	1:10	568:1	1.4:1
3 Au/B2	21:1	1:7	604:1	2.0:1

<sup>[a]</sup> Composition calculated from the metal content and ionic liquid content values determined by XRF and CHN Elemental Analysis, respectively; <sup>[b]</sup> Surface composition calculated on basis of the Au 4f, N 1s and Si 2p measured by XPS; <sup>[c]</sup> Surface composition calculated on the basis of the Au 4f, Al 2p and O 1s measured by XPS.

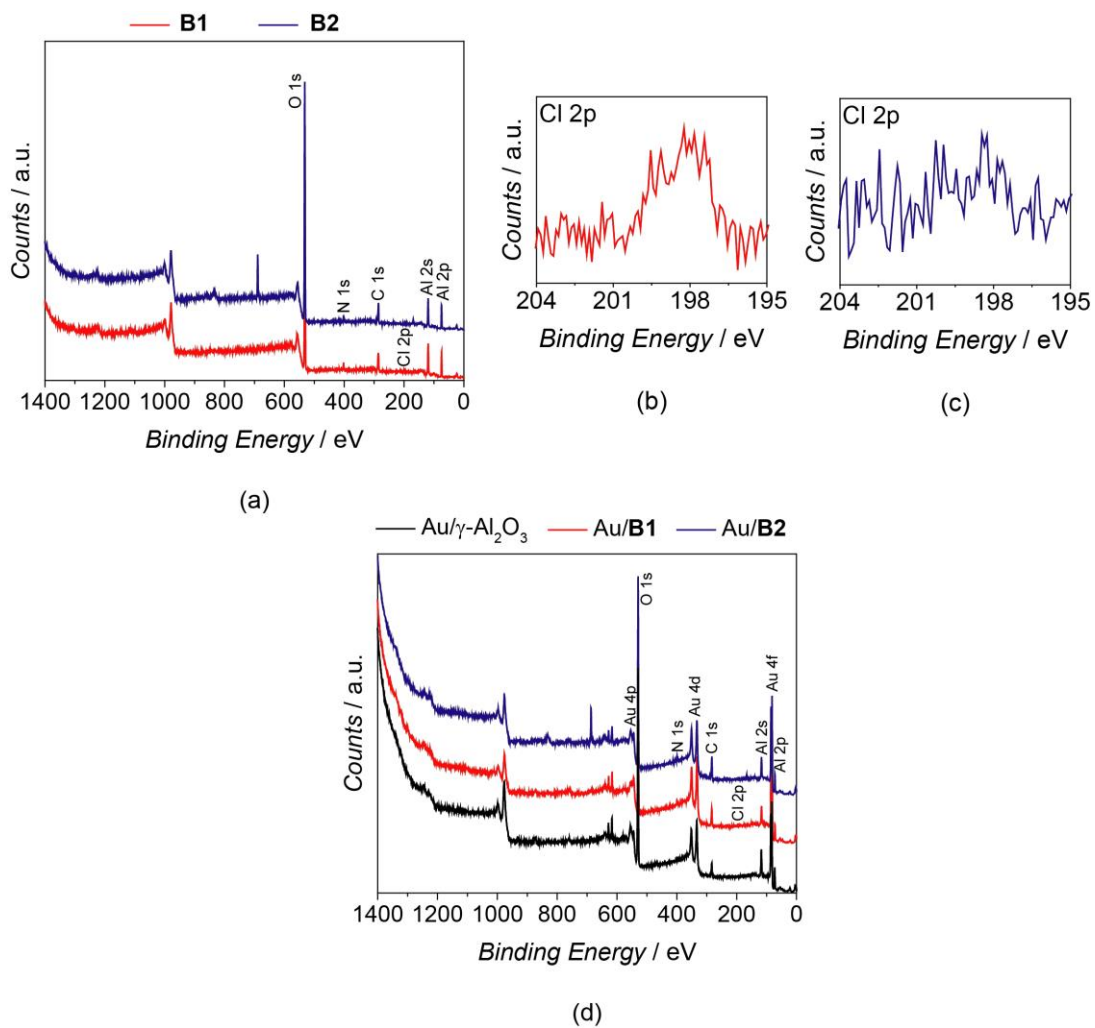


**Figure S7.** XPS (a) at the long scan region of the **B1** and **B2** supports, high resolution at Cl 2p region of the (b) **B1** support and (c) **B2** support, and (d) at the long scan region of the Au/Al<sub>2</sub>O<sub>3</sub>, Au/**B1** and Au/**B2** catalysts.

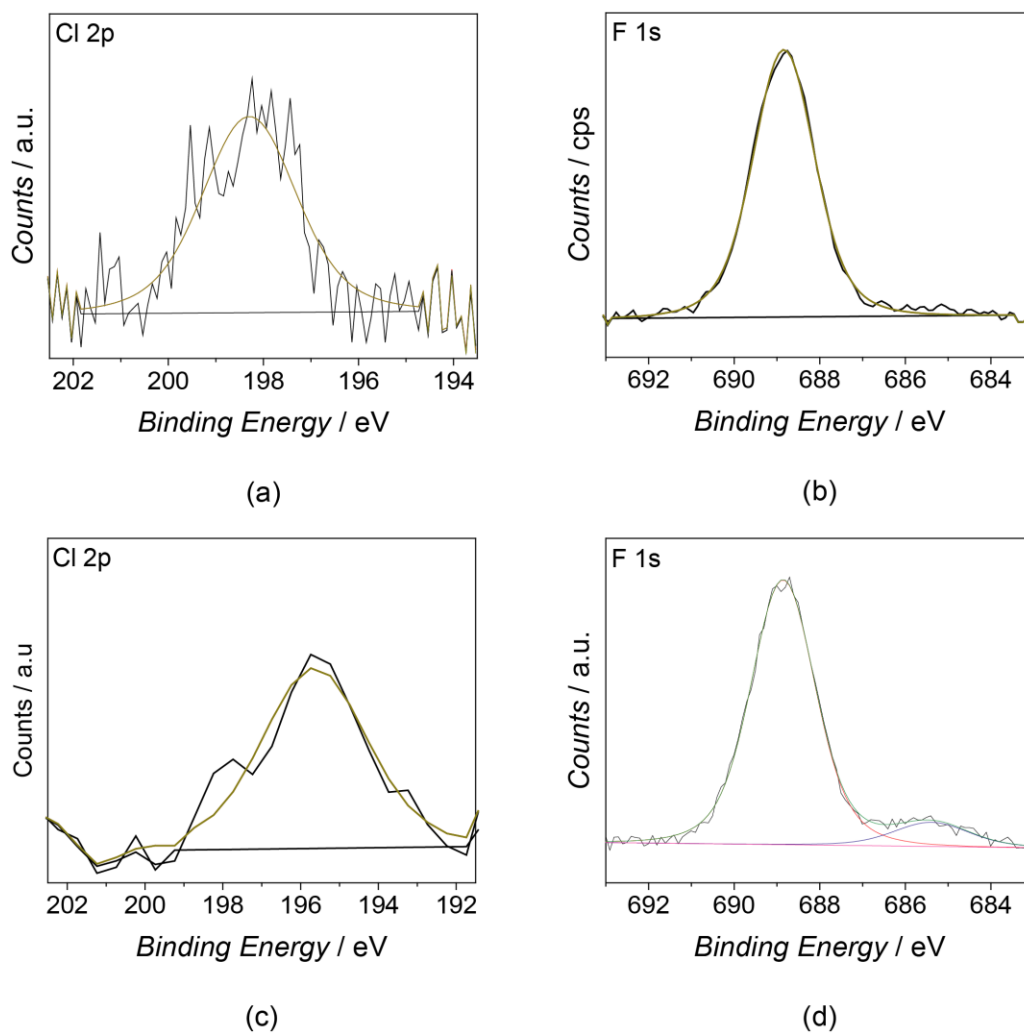


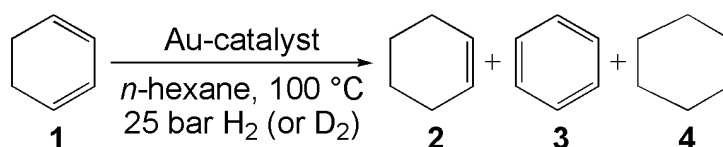
**Figure S8.** XPS measurements at Cl and F regions for the (a) **B1**, (b) **B2** supports and (c) Au/**B1** and (d) Au/**B2** catalysts.

## Section 8.

### **Results Discussion: Hydrogenation and Disproportionation of 1,3-Cyclohexadiene Catalyzed by AuNPs Under H<sub>2</sub> or D<sub>2</sub> atmosphere.**

It is demonstrated that the IL layer influences the catalytic performance of the 1,3-cyclohexadiene hydrogenation by improving the product selectivity and by decreasing the catalytic activity (Table 2). The Au/B1 and Au/B2 catalysts required much higher hydrogen pressures and temperature pressures than Au/ $\gamma$ -Al<sub>2</sub>O<sub>3</sub> catalyst once the IL layers are surrounding the AuNPs. The controlling of the access of the reagents to the Au-surface by the IL layer avoids their interaction with the Al<sub>2</sub>O<sub>3</sub> (the interaction that facilitates the H<sub>2</sub> activation). The ability of the support to help in the heterolytic dissociation of H<sub>2</sub> has a direct dependence on the catalyst activity and an indirect dependence with the particle size.<sup>111,114-116</sup>

**Table S9.** Hydrogenation and disproportionation of 1,3-cyclohexadiene under H<sub>2</sub> or D<sub>2</sub> atmosphere catalyzed by AuNPs.



Entry <sup>[a,b]</sup>	Catalyst	2-d <sub>0</sub> /	2-d <sub>2</sub> <sup>1,2</sup> /	2-d <sub>2</sub> <sup>1,4</sup> /	3-d <sub>0</sub> /	4/	4-d <sub>4</sub> /	TOF <sup>[c]</sup> / min <sup>-1</sup>
		%	%	%	%	%	%	
1	Au/ $\gamma$ -Al <sub>2</sub> O <sub>3</sub>	89	—	—	1	10	—	6.9
2 <sup>[d]</sup>	Au/ $\gamma$ -Al <sub>2</sub> O <sub>3</sub>	1	72	18	1	—	8	6.1
3	Au/B1	93	—	—	2	5	—	3.2
4 <sup>[d]</sup>	Au/B1	3	74	16	3	—	4	0.7
5	Au/B2	96	—	—	2	2	—	4.1
6 <sup>[d]</sup>	Au/B2	2	80	15	2	—	1	1.1

<sup>[a]</sup> Reaction conditions: Au (0.5  $\mu$ mol), 1,3-cyclohexadiene/Au = 250, *n*-hexane (5 mL), 25 bar H<sub>2</sub> or D<sub>2</sub>, 100 °C and 250 rpm; <sup>[b]</sup> Conversion and selectivity at conversions >99% determined by GC analysis; <sup>[c]</sup> TOF defined as mol substrate converted/(mol Au surface  $\times$  minute) calculated from the slope of plots of TON vs. time at low substrate conversions;<sup>137</sup> <sup>[d]</sup> D<sub>2</sub> instead of H<sub>2</sub>.

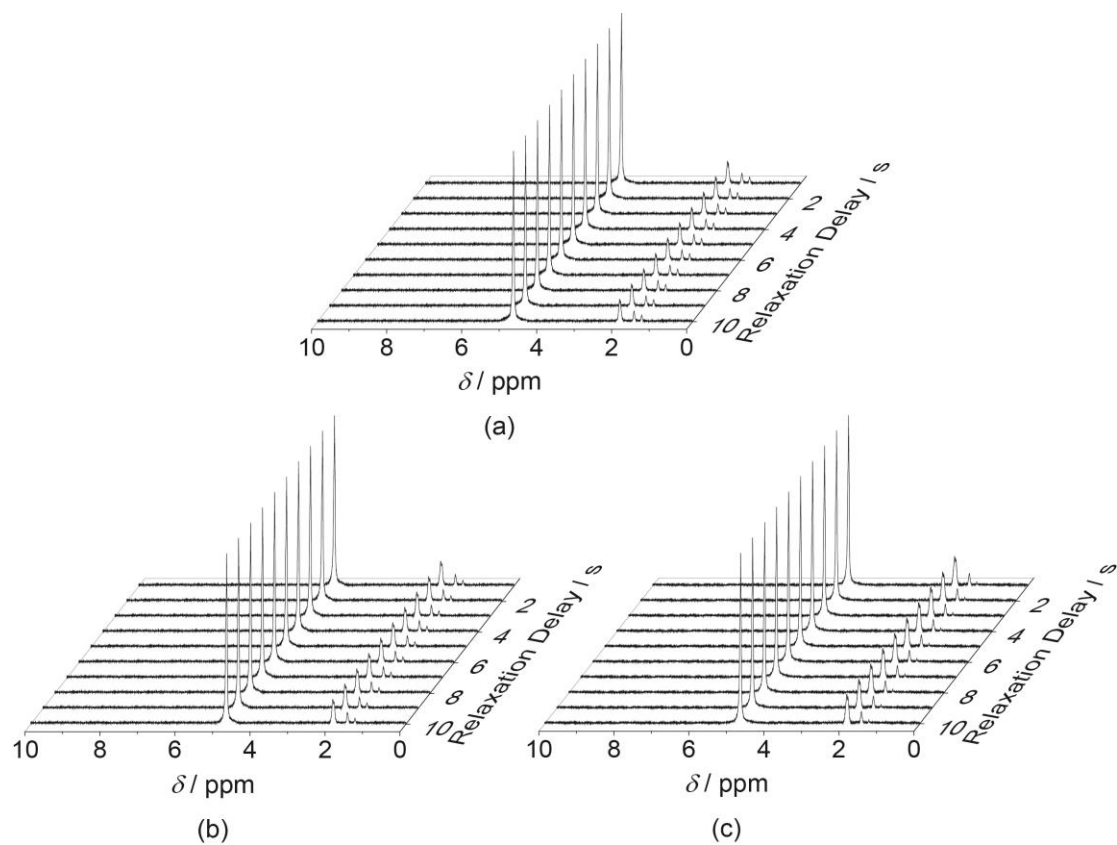


**Figure S9.**  $^2\text{H}$  NMR ( $\text{D}_2\text{O}$ ) spectra of the reaction products formed by hydrogenation of the 1,3-cyclohexadiene with  $\text{D}_2$  catalyzed by (a)  $\text{Au}/\gamma\text{-Al}_2\text{O}_3$ , (b)  $\text{Au}/\mathbf{B1}$  and (c)  $\text{Au}/\mathbf{B2}$  catalysts.

## Section S9.

### Results Discussion: Selective Hydrogenations Catalyzed by Au/B2.

**Table S10.** Selective hydrogenation of 1,3-dienes, alkenes conjugated with an arene system, internal aliphatic alkynes and  $\alpha,\beta$ -unsaturated carbonyl compounds catalyzed by Au/B2 under optimized reaction conditions.

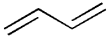
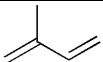
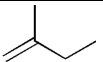
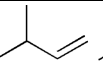
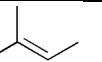
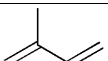
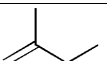
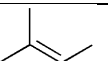
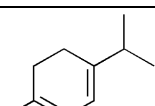
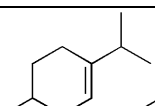
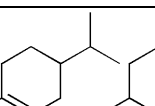
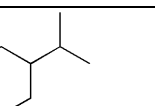
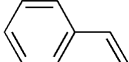
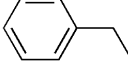
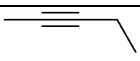
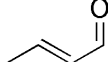
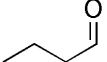
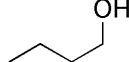
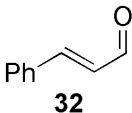
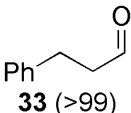
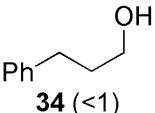
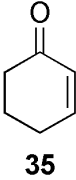
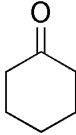
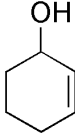
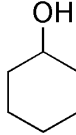
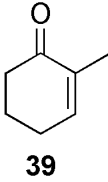
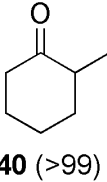
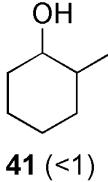
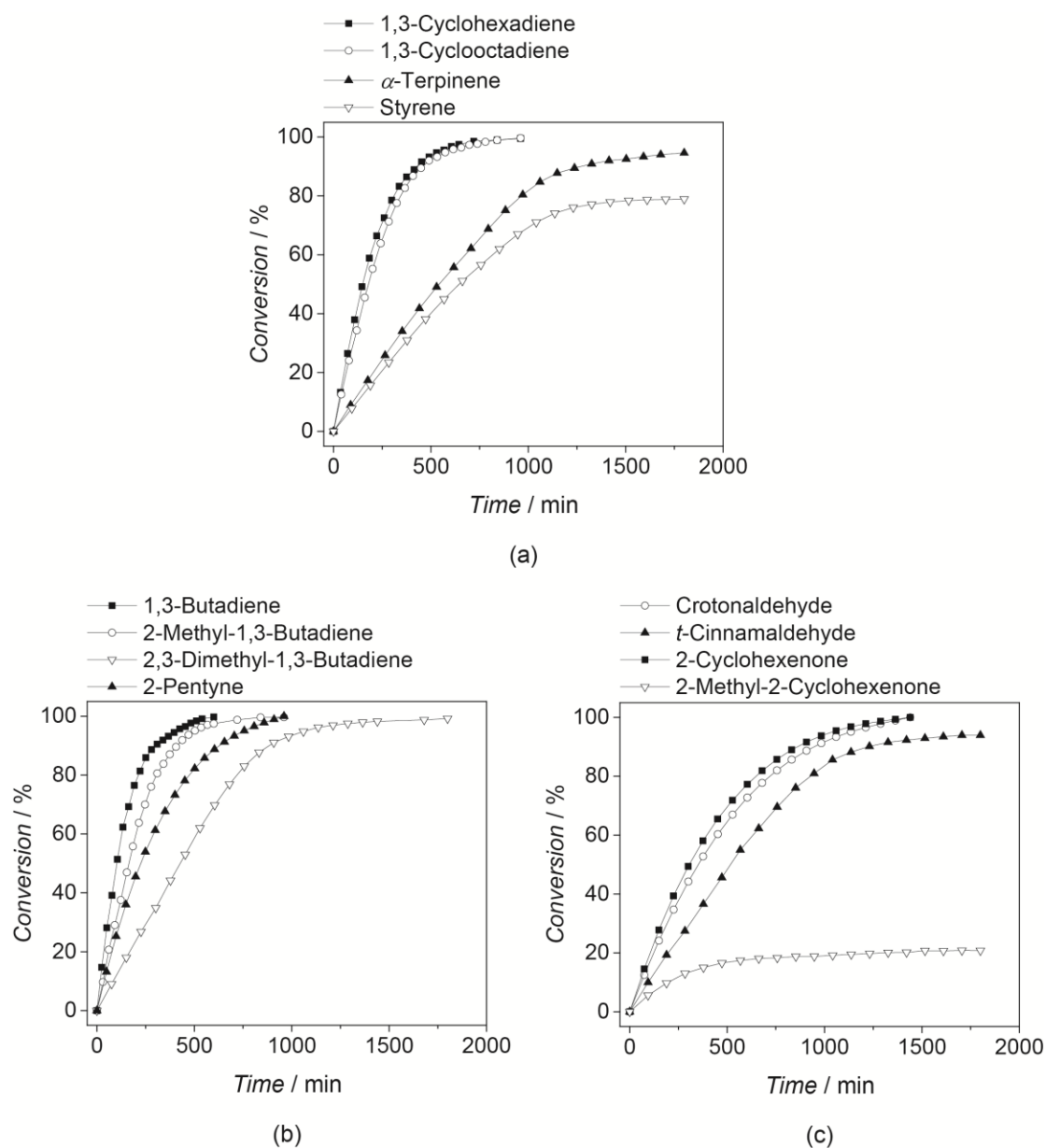
Entry <sup>[a,b]</sup>	Substrate	Conversion/ % [t/ h]	Products (Selectivity/ %)	TOF <sup>[c]</sup> / min <sup>-1</sup>
1	 <b>1</b>	>99 [16]	   <b>2</b> (96) <b>3</b> (2) <b>4</b> (2)	4.1
2	 <b>5</b>	>99 [16]	  <b>6</b> (98) <b>7</b> (2)	3.3
3	 <b>8</b>	>99 [10]	    <b>9</b> (52) <b>10</b> (33) <b>11</b> (12) <b>12</b> (3)	6.5
4	 <b>13</b>	>99 [16]	   <b>14</b> (27) <b>15</b> (15) <b>16</b> (58)	3.5
5	 <b>17</b>	>99 [30]	  <b>18</b> (29) <b>19</b> (71)	1.3
6	 <b>20</b>	96 [30]	   <b>21</b> (76) <b>22</b> (22) <b>23</b> (2)	1.1
7	 <b>24</b>	79 [30]	 <b>25</b> (>99)	0.9
8	 <b>26</b>	>99 [16]	  <b>27</b> (27) <b>28</b> (73)	2.9
9	 <b>29</b>	>99 [24]	  <b>30</b> (95) <b>31</b> (5)	1.8

Table S10. (cont.)

10		94 [30]	 	1.0
11		>99 [24]	  	2.1
12		21 [30]	 	0.6

<sup>[a]</sup> Reaction conditions: Au (0.5  $\mu\text{mol}$ ), substrate/Au = 250, 5 mL of solvent (*n*-hexane for dienes and alkynes, and *m*-xylene for  $\alpha,\beta$ -unsaturated carbonyl compounds), 25 bar  $\text{H}_2$ , 100  $^\circ\text{C}$  and 250 rpm; <sup>[b]</sup> Selectivity determined at conversions >99% by GC analysis; <sup>[c]</sup> TOF = mol substrate converted/(mol Au surface  $\times$  minute) calculated from the slope of plots of TON vs. time at low substrate conversions.



**Figure S10.** Selective hydrogenation of the (a) 1,3-cyclohexadiene; 1,3-cyclooctadiene;  $\alpha$ -terpinene; styrene, (b) 1,3-butadiene; 2-methyl-1,3-butadiene; 2,3-dimethyl-1,3-butadiene; 2-pentyne and (c) crotonaldehyde; *t*-cinnamaldehyde; 2-cyclohexenone; 2-methyl-2-cyclohexenone by Au/B<sub>2</sub> catalyst under optimized reaction conditions.

## Section S10.

### **Results Discussion:** Kinetic Experiments on the 1,3-Cyclooctadiene Hydrogenation under H<sub>2</sub> atmosphere catalyzed by AuNPs.

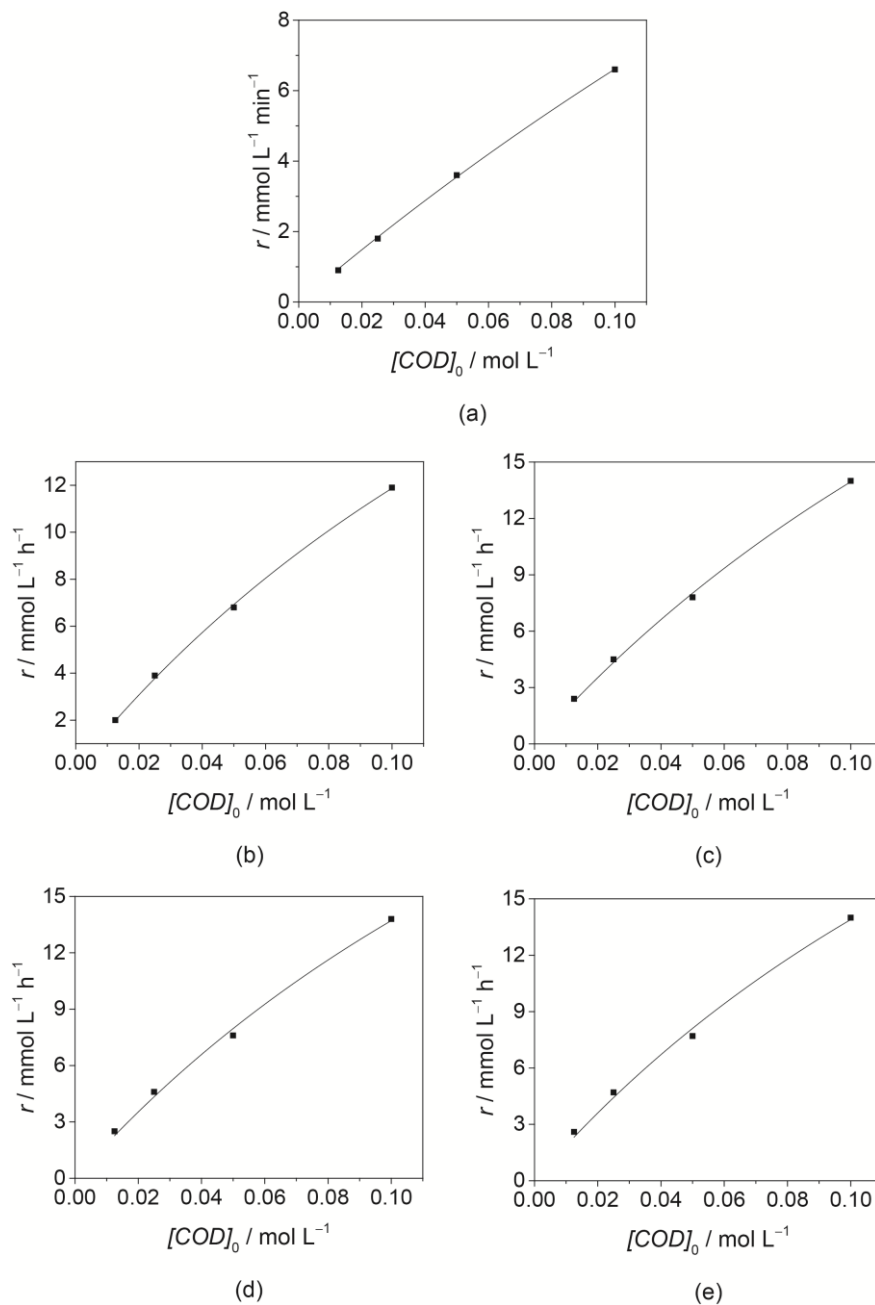
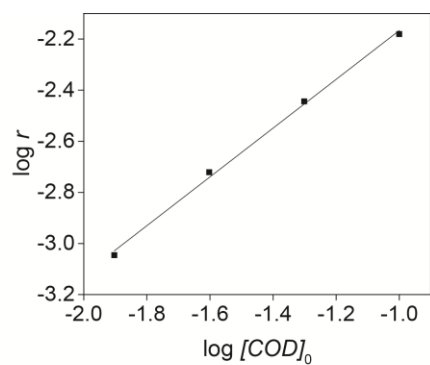
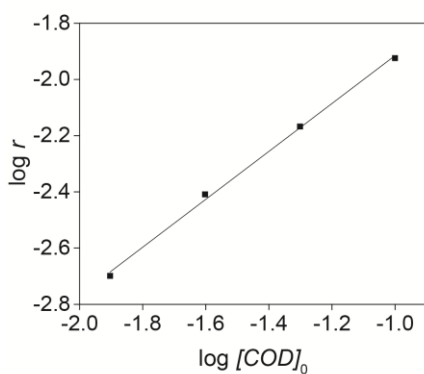


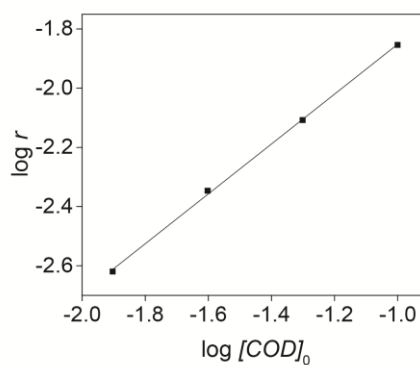
**Figure S11.** Reaction rate dependence on substrate concentrations at hydrogen pressures: (a) 10 bar, (b) 15 bar, (c) 20 bar, (d) 25 bar and (e) 30 bar.



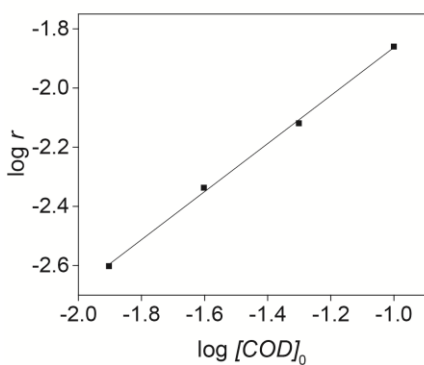
(a)



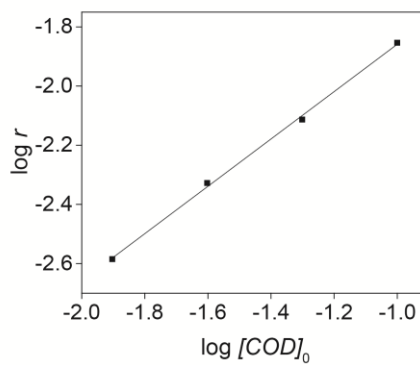
(b)



(c)



(d)



(e)

**Figure S12.** Reaction rate logarithm dependence on substrate concentrations at hydrogen pressures: (a) 10 bar, (b) 15 bar, (c) 20 bar, (d) 25 bar and (e) 30 bar.

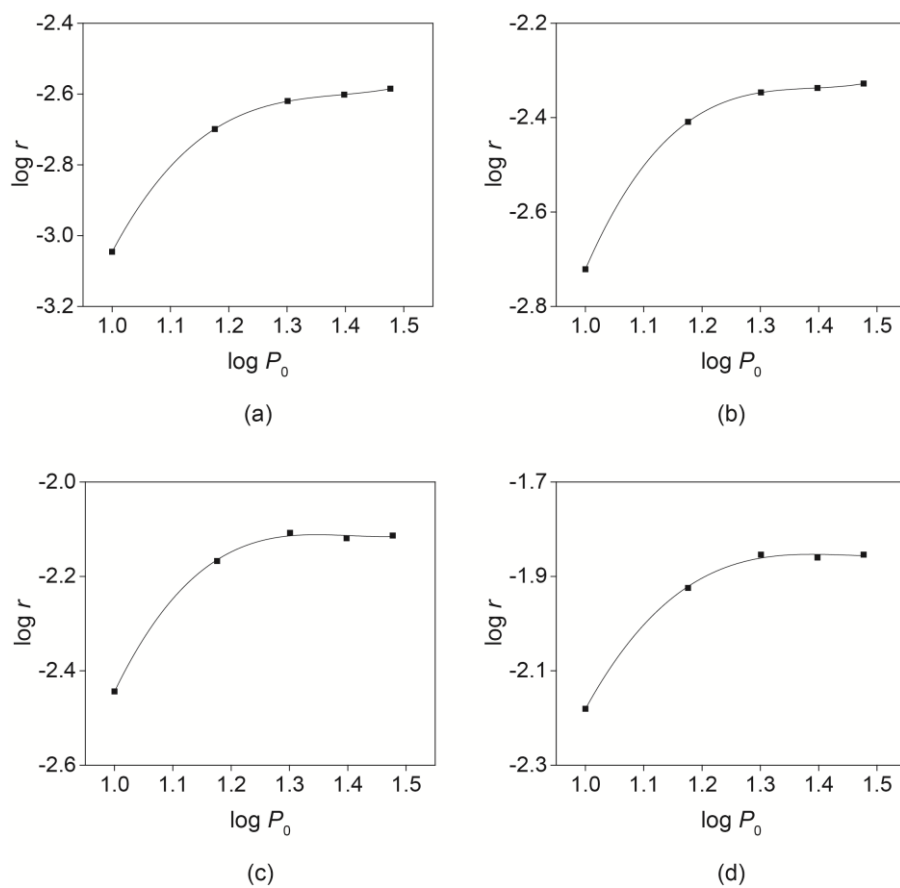


**Figure S13.** Reaction rate logarithm dependence on hydrogen pressure at initial 1,3-cyclooctadiene concentrations: (a) 0.0125 mol L<sup>-1</sup>, (b) 0.025 mol L<sup>-1</sup>, (c) 0.050 mol L<sup>-1</sup> and (d) 0.100 mol L<sup>-1</sup>.

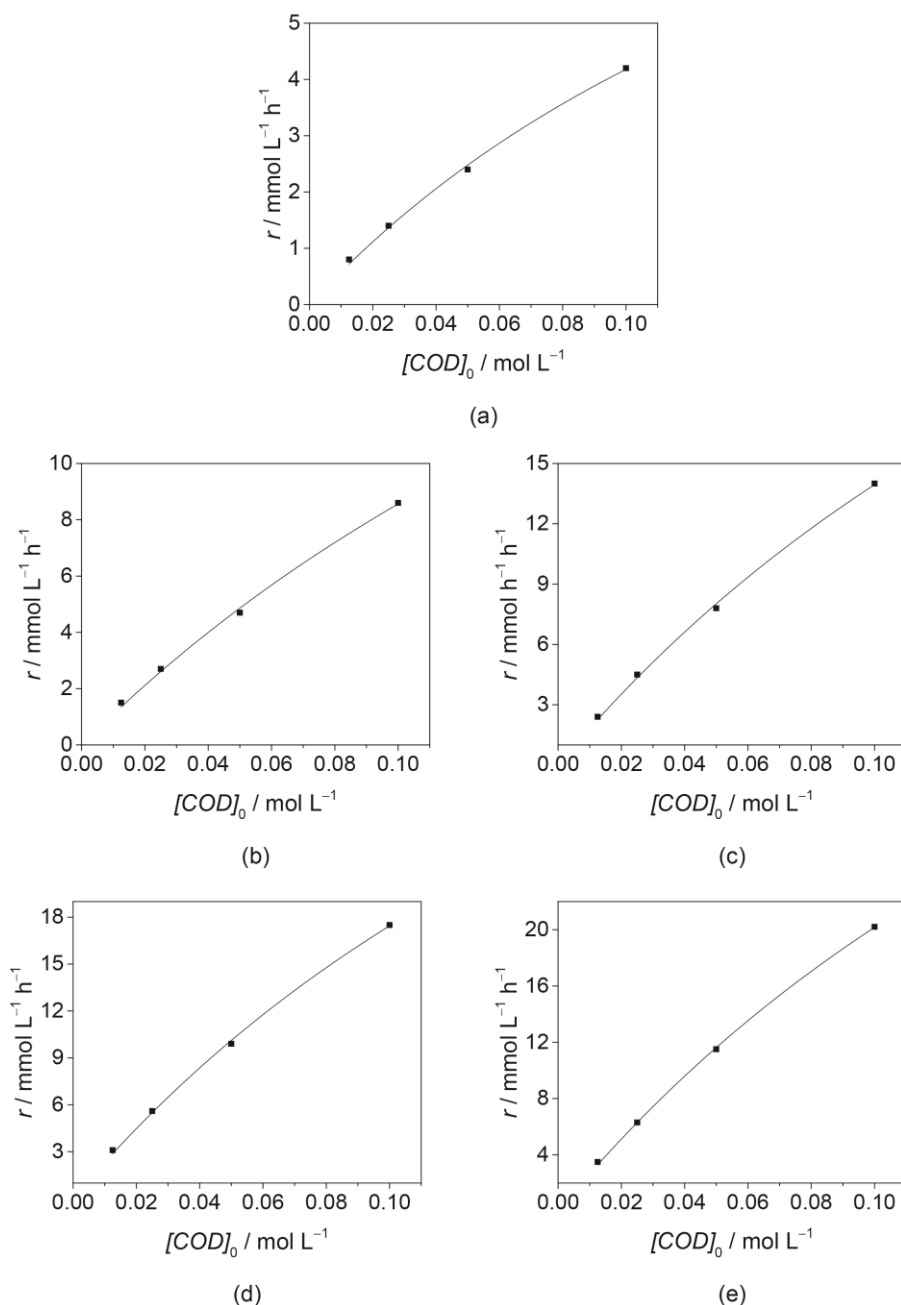
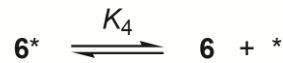
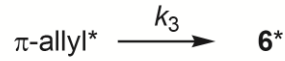
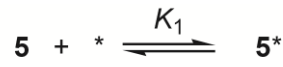


**Figure S14.** Reaction rate dependence on substrate concentrations at temperatures: (a) 50 °C, (b) 75 °C, (c) 100 °C, (d) 125 °C and (e) 150 °C.

We proposed that according to Scheme 4, the substrate 1,3-cyclooctadiene (**5**) interacts with the AuNPs surface to form the adsorbed species which reacts with  $\text{H}_2$  to form the  $\pi$ -allyl intermediate and the final product cyclooctene (**6**). Thus,  $k_1$  and  $k_4$  are the kinetic constants for adsorption and  $k_{-1}$  and  $k_{-4}$  the kinetic constants for desorption of the substrate and product, respectively and  $k_2$  and  $k_3$  the surface rate constants (combined

into  $k_r$ ). The RDS is the H<sub>2</sub> and substrate competitive adsorption/activation on the same active sites:



$$K_1 = \frac{k_1}{k_{-1}} = \frac{[5^*]}{[5][*]}$$

$$K_2 = \frac{k_2}{k_{-2}} = \frac{[\pi\text{-allyl}^*]}{[5^*]}$$

$$K_4 = \frac{k_4}{k_{-4}} = \frac{[6^*]}{[6][*]}$$

$$r = k_3 [\pi\text{-allyl}^*] = k_3 K_2 [5^*] = \frac{k_r K_1 [5][*]_0}{1 + K_1 [5] + K_4 [6]} \quad (\text{Eq. S1})$$

In this case, it is assumed that six is not adsorbed on the AuNPs surface in a kinetically significant amount and, thus,  $[6] \gg [6^*]$  leading to  $K_4 \rightarrow 0$  and the following surface mass balance:

$$[*]_0 = [5^*] + [*]$$

The total surface area of NPs normalized to the unit volume of the reaction medium ( $[*]_0$ ) is 0.93 m<sup>2</sup> L<sup>-1</sup> and the rate of the reaction expressed by:

$$r = k_r [5^*] = \frac{k_r K_1 [5][*]_0}{1 + K_1 [5]} \quad (\text{Eq. S2})$$

with  $k_3$  and  $K_2$  combined into  $k_r$  as the overall surface reaction and intermediate adsorption.

**Table S11.** Kinetic parameters ( $k_r$  and  $K_1$ ) in the selective hydrogenation of the 1,3-cyclooctadiene by Au/B2 catalyst at different pressures.

Entry <sup>[a]</sup>	P <sub>H2</sub> / bar	$k_r^{[b,c]}$ / mol m <sup>-2</sup> h <sup>-1</sup>	$K_1^{[c]}$ / L mol <sup>-1</sup>
1	10	0.052	1.58
2	15	0.045	3.99
3	20	0.058	3.54
4	25	0.053	3.87
5	30	0.052	4.00

<sup>[a]</sup> Reaction conditions: Au (0.5 μmol), 1,3-cyclohexadiene/Au = 250, *n*-hexane (5 mL), 100 °C and 250 rpm; <sup>[b]</sup> Rate constant normalized to the total surface area of the nanoparticles per unit of volume; <sup>[c]</sup> Determined by mathematical non-linear fitting of the experimental data.

**Table S12.** Kinetic parameters ( $k_r$  and  $K_1$ ) in the selective hydrogenation of the 1,3-cyclooctadiene by Au/B2 catalyst at various temperatures.

Entry <sup>[a]</sup>	T/ °C	$k_r^{[b,c]}$ / mol m <sup>-2</sup> h <sup>-1</sup>	$K_1^{[c]}$ / L mol <sup>-1</sup>
1	50	0.014	4.57
2	75	0.038	3.13
3	100	0.058	3.54
4	125	0.068	3.81
5	150	0.081	3.61

<sup>[a]</sup> Reaction conditions: Au (0.5 μmol), 1,3-cyclohexadiene/Au = 250, *n*-hexane (5 mL), 20 bar H<sub>2</sub> and 250 rpm; <sup>[b]</sup> Rate constant normalized to the total surface area of the nanoparticles per unit of volume; <sup>[c]</sup> Determined by mathematical non-linear fitting of the experimental data.

## 10. References.

- (1) Vile, G.; Perez-Ramirez, J. *Nanoscale* **2014**, *6*, 13476-13482.
- (2) Gluhoi, A. C.; Bakker, J. W.; Nieuwenhuys, B. E. *Catal. Today* **2010**, *154*, 13-20.
- (3) Segura, Y.; Lopez, N.; Perezramirez, J. *J. Catal.* **2007**, *247*, 383-386.
- (4) Zhang, X.; Shi, H.; Xu, B.-Q. *J. Catal.* **2011**, *279*, 75-87.
- (5) Yang, X.-F.; Wang, A.-Q.; Wang, Y.-L.; Zhang, T.; Li, J. *J. Phys. Chem. C* **2010**, *114*, 3131-3139.
- (6) Hugon, A.; Kolli, N. E.; Louis, C. *J. Catal.* **2010**, *274*, 239-250.
- (7) Zhang, X.; Shi, H.; Xu, B.-Q. *Catal. Today* **2007**, *122*, 330-337.
- (8) Zhang, X.; Shi, H.; Xu, B. Q. *Angew. Chem. Int. Ed.* **2005**, *44*, 7132-7135.
- (9) Guan, Y.; Hensen, E. J. M. *Phys. Chem. Chem. Phys.* **2009**, *11*, 9578-9582.

- (10) Guan, Y.; Lighthart, D. A. J. M.; Pirgon-Galin, Ö.; Pieterse, J. A. Z.; Santen, R. A.; Hensen, E. J. M. *Top. Catal.* **2011**, *54*, 424-438.
- (11) Zhang, X.; Guo, Y. C.; Zhang, Z. C.; Gao, J. S.; Xu, C. M. *J. Catal.* **2012**, *292*, 213-226.
- (12) Castillejos, E.; Bachiller-Baeza, B.; Asedegbega-Nieto, E.; Guerrero-Ruiz, A.; Rodríguez-Ramos, I. *RSC Adv.* **2015**, *5*, 81583-81598.
- (13) Lozano-Martin, M. C.; Castillejos, E.; Bachiller-Baeza, B.; Rodríguez-Ramos, I.; Guerrero-Ruiz, A. *Catal. Today* **2015**, *249*, 117-126.
- (14) Zhang, X.; Llabrés i Xamena, F. X.; Corma, A. *J. Catal.* **2009**, *265*, 155-160.
- (15) Oumahi, C.; Lombard, J.; Casale, S.; Calers, C.; Delannoy, L.; Louis, C.; Carrier, X. *Catal. Today* **2014**, *235*, 58-71.
- (16) Dash, P.; Dehm, N. A.; Scott, R. W. J. *J. Mol. Catal. A* **2008**, *286*, 114-119.
- (17) Nikolaev, S. A.; Smirnov, V. V. *Catal. Today* **2009**, *147*, Supplement, S336-S341.
- (18) Shao, L. D.; Huang, X.; Teschner, D.; Zhang, W. *ACS Catal.* **2014**, *4*, 2369-2373.
- (19) Li, G.; Jin, R. C. *J. Am. Chem. Soc.* **2014**, *136*, 11347-11354.
- (20) Liang, S. Z.; Hammond, G. B.; Xu, B. *Chem. Commun.* **2016**, *52*, 6013-6016.
- (21) Mitsudome, T.; Yamamoto, M.; Maeno, Z.; Mizugaki, T.; Jitsukawa, K.; Kaneda, K. *J. Am. Chem. Soc.* **2015**, *137*, 13452-13455.
- (22) Schimpf, S.; Lucas, M.; Mohr, C.; Rodemerck, U.; Brückner, A.; Radnik, J.; Hofmeister, H.; Claus, P. *Catal. Today* **2002**, *72*, 63-78.
- (23) Claus, P.; Bruckner, A.; Mohr, C.; Hofmeister, H. *J. Am. Chem. Soc.* **2000**, *122*, 11430-11439.
- (24) Claus, P.; Bruckner, A.; Mohr, C.; Hofmeister, H. *J. Am. Chem. Soc.* **2000**, *122*, 11430-11439.
- (25) Zanella, R.; Louis, C.; Giorgio, S.; Touroude, R. *J. Catal.* **2004**, *223*, 328-339.
- (26) Zhu, Y.; Tian, L.; Jiang, Z.; Pei, Y.; Xie, S. H.; Qiao, M. H.; Fan, K. N. *J. Catal.* **2011**, *281*, 106-118.
- (27) Chatterjee, M.; Ikushima, Y.; Hakuta, Y.; Kawanami, H. *Adv. Synth. Catal.* **2006**, *348*, 1580-1590.
- (28) Chatterjee, M.; Ikushima, Y. *Stud. Surf. Sci. Catal.* **2005**, *156*, 427-432.
- (29) Pei, Y.; Guo, P. J.; Zhu, L. J.; Yan, S. R.; Qiao, M. H.; Fan, K. N. *Stud. Surf. Sci. Catal.* **2007**, *170*, 1174-1181.
- (30) Zhong, R. Y.; Yan, X. H.; Gao, Z. K.; Zhang, R. J.; Xu, B. Q. *Catal. Sci. Technol.* **2013**, *3*, 3013-3019.
- (31) Hong, Y. C.; Sun, K. Q.; Zhang, G. R.; Zhong, R. Y.; Xu, B. Q. *Chem. Commun.* **2011**, *47*, 1300-1302.
- (32) Shi, H.; Xu, N.; Zhao, D.; Xu, B. Q. *Catal. Commun.* **2008**, *9*, 1949-1954.
- (33) Sun, K. Q.; Hong, Y. C.; Zhang, G. R.; Xu, B. Q. *ACS Catal.* **2011**, *1*, 1336-1346.
- (34) Bus, E.; Prins, R.; van Bokhoven, J. A. *Catal. Commun.* **2007**, *8*, 1397-1402.
- (35) Castillejos, E.; Gallegos-Suarez, E.; Bachiller-Baeza, B.; Bacsá, R.; Serp, P.; Guerrero-Ruiz, A.; Rodríguez-Ramos, I. *Catal. Commun.* **2012**, *22*, 79-82.
- (36) Milone, C.; Crisafulli, C.; Ingoglia, R.; Schipilliti, L.; Galvagno, S. *Catal. Today* **2007**, *122*, 341-351.
- (37) Milone, C.; Ingoglia, R.; Schipilliti, L.; Crisafulli, C.; Neri, G.; Galvagno, S. *J. Catal.* **2005**, *236*, 80-90.
- (38) Fujiwara, S.; Takanashi, N.; Nishiyabu, R.; Kubo, Y. *Green Chem.* **2014**, *16*, 3230-3236.
- (39) Biondi, I.; Laurenczy, G.; Dyson, P. J. *Inorg. Chem.* **2011**, *50*, 8038-8045.
- (40) Cano, I.; Huertos, M. A.; Chapman, A. M.; Buntkowsky, G.; Gutmann, T.; Groszewicz, P. B.; van Leeuwen, P. W. N. M. *J. Am. Chem. Soc.* **2015**, *137*, 7718-7727.
- (41) Cano, I.; Chapman, A. M.; Urakawa, A.; van Leeuwen, P. W. *J. Am. Chem. Soc.* **2014**, *136*, 2520-2528.
- (42) Mertens, P. G. N.; Poelman, H.; Ye, X.; Vankelecom, I. F. J.; Jacobs, P. A.; De Vos, D. E. *Catal. Today* **2007**, *122*, 352-360.
- (43) Mertens, P. G. N.; Vandezande, P.; Ye, X.; Poelman, H.; Vankelecom, I. F. J.; De Vos, D. E. *Appl. Catal. A* **2009**, *355*, 176-183.
- (44) Zhu, Y.; Qian, H.; Drake, B. A.; Jin, R. *Angew. Chem. Int. Ed.* **2010**, *49*, 1295-1298.
- (45) Turner, M.; Golovko, V. B.; Vaughan, O. P. H.; Abdulkin, P.; Berenguer-Murcia, A.; Tikhov, M. S.; Johnson, B. F. G.; Lambert, R. M. *Nature* **2008**, *454*, 981-983.

- (46) Boronat, M.; Concepcion, P.; Corma, A.; Gonzalez, S.; Illas, F.; Serna, P. *J. Am. Chem. Soc.* **2007**, *129*, 16230-16237.
- (47) Corma, A.; Serna, P.; Garcia, H. *J. Am. Chem. Soc.* **2007**, *129*, 6358-6359.
- (48) Cortright, R. D.; Dumesic, J. A. In *Advances in Catalysis*; Academic Press: 2001; Vol. Volume 46, p 161.
- (49) Murzin, D. Y. *Chem. Eng. Sci.* **2009**, *64*, 1046-1052.
- (50) Serna, P.; Concepción, P.; Corma, A. *J. Catal.* **2009**, *265*, 19-25.
- (51) Bus, E.; Miller, J. T.; van Bokhoven, J. A. *J. Phys. Chem. B* **2005**, *109*, 14581-14587.
- (52) Buchanan, D. A.; Webb, G. *J. Chem. Soc., Faraday Trans. 1* **1975**, *71*, 134-144.
- (53) Hugon, A.; Delannoy, L.; Louis, C. *Gold Bull.* **2009**, *42*, 310-320.
- (54) Jia, J.; Haraki, K.; Kondo, J. N.; Domen, K.; Tamaru, K. *J. Phys. Chem. B* **2000**, *104*, 11153-11156.
- (55) Liu, X.; Mou, C.-Y.; Lee, S.; Li, Y.; Secret, J.; Jang, B. W. L. *J. Catal.* **2012**, *285*, 152-159.
- (56) Azizi, Y.; Petit, C.; Pitchon, V. *J. Catal.* **2008**, *256*, 338-344.
- (57) Bond, G. C.; Sermon, P. A.; Webb, G.; Buchanan, D. A.; Wells, P. B. *J. Chem. Soc., Chem. Commun.* **1973**, 444-445.
- (58) Erkelens, J.; Kemball, C.; Galwey, A. K. *Trans. Faraday Soc.* **1963**, *59*, 1181-1191.
- (59) Wilson, J. N.; Otvos, J. W.; Stevenson, D. P.; Wagner, C. D. *Ind. Eng. Chem.* **1953**, *45*, 1480-1487.
- (60) Sachtler, W. M. H.; Boer, N. H. d. *J. Phys. Chem.* **1960**, *64*, 1579-1580.
- (61) Kubas, G. J. *Chem. Rev.* **2007**, *107*, 4152-4205.
- (62) Bullock, R. M.; Rappoli, B. J. *J. Chem. Soc., Chem. Commun.* **1989**, 1447-1448.
- (63) Bullock, R. M.; Song, J.-S.; Szalda, D. J. *Organometallics* **1996**, *15*, 2504-2516.
- (64) Bullock, R. M.; Voges, M. H. *J. Am. Chem. Soc.* **2000**, *122*, 12594-12595.
- (65) Voges, M. H.; Bullock, R. M. *J. Chem. Soc., Dalton Trans.* **2002**, 759-770.
- (66) Magee, M. P.; Norton, J. R. *J. Am. Chem. Soc.* **2001**, *123*, 1778-1779.
- (67) Corma, A.; Boronat, M.; Gonzalez, S.; Illas, F. *Chem. Comm.* **2007**, 3371-3373.
- (68) Andrews, L. *Chem. Soc. Rev.* **2004**, *33*, 123-132.
- (69) Mohr, C.; Hofmeister, H.; Radnik, J.; Claus, P. *J. Am. Chem. Soc.* **2003**, *125*, 1905-1911.
- (70) Boronat, M.; Concepción, P.; Corma, A. *J. Phys. Chem. C* **2009**, *113*, 16772-16784.
- (71) Boronat, M.; Illas, F.; Corma, A. *J. Phys. Chem. A* **2009**, *113*, 3750-3757.
- (72) Barton, D. G.; Podkolzin, S. G. *J. Phys. Chem. B* **2005**, *109*, 2262-2274.
- (73) Kartusch, C.; Bokhoven, J. A. *Gold Bull.* **2009**, *42*, 343-348.
- (74) Gluhoi, A. C.; Vreeburg, H. S.; Bakker, J. W.; Nieuwenhuys, B. E. *Appl. Catal. A* **2005**, *291*, 145-150.
- (75) Abad, A.; Corma, A.; García, H. *Chem. Eur. J.* **2008**, *14*, 212-222.
- (76) Fountoulaki, S.; Daikopoulou, V.; Gkizis, P. L.; Tamiolakis, I.; Armatas, G. S.; Lykakis, I. N. *ACS Catal.* **2014**, *4*, 3504-3511.
- (77) He, L.; Wang, L.-C.; Sun, H.; Ni, J.; Cao, Y.; He, H.-Y.; Fan, K.-N. *Angew. Chem. Int. Ed.* **2009**, *48*, 9538-9541.
- (78) Petkov, V.; Peng, Y.; Williams, G.; Huang, B.; Tomalia, D.; Ren, Y. *Phys. Rev. B* **2005**, *72*, 195402.
- (79) Zhu, J.; Kónya, Z.; Puentes, V. F.; Kiricsi, I.; Miao, C. X.; Ager, J. W.; Alivisatos, A. P.; Somorjai, G. A. *Langmuir* **2003**, *19*, 4396-4401.
- (80) Van Santen, R. A. *Acc. Chem. Res.* **2009**, *42*, 57-66.
- (81) Henry, C. R. *Surf. Sci. Rep.* **1998**, *31*, 231-235.
- (82) Borodziński, A.; Bonarowska, M. *Langmuir* **1997**, *13*, 5613-5620.
- (83) Van Hardeveld, R.; Hartog, F. *Surf. Sci.* **1969**, *15*, 189-230.
- (84) Zhou, X.; Xu, W.; Liu, G.; Panda, D.; Chen, P. *J. Am. Chem. Soc.* **2010**, *132*, 138-146.
- (85) Cardenas-Lizana, F.; Gomez-Quero, S.; Idriss, H.; Keane, M. A. *J. Catal.* **2009**, *268*, 223-234.
- (86) Panigrahi, S.; Basu, S.; Praharaj, S.; Pande, S.; Jana, S.; Pal, A.; Ghosh, S. K.; Pal, T. *J. Phys. Chem. C* **2007**, *111*, 4596-4605.
- (87) Mohr, C.; Hofmeister, H.; Claus, P. *J. Catal.* **2003**, *213*, 86-94.
- (88) Moulder, J. F.; Chastain, J. *Handbook of X-ray Photoelectron Spectroscopy: A Reference Book of Standard Spectra for Identification and Interpretation of XPS Data*; Physical Electronics: Minneapolis, MN, 1995.

- (89) Citrin, P. H.; Wertheim, G. K. *Phys. Rev. B* **1983**, *27*, 3176-3200.
- (90) Palgrave, R. G.; Parkin, I. P. *J. Am. Chem. Soc.* **2006**, *128*, 1587-1597.
- (91) Gucci, L.; Petö, G.; Beck, A.; Frey, K.; Geszti, O.; Molnár, G.; Daróczi, C. *J. Am. Chem. Soc.* **2003**, *125*, 4332-4337.
- (92) Brodersen, S. H.; Grønberg, U.; Hvolbæk, B.; Schiøtz, J. *J. Catal.* **2011**, *284*, 34-41.
- (93) Overbury, S. H.; Schwartz, V.; Mullins, D. R.; Yan, W.; Dai, S. *J. Catal.* **2006**, *241*, 56-65.
- (94) Bond, G. C. *Faraday Discuss.* **2011**, *152*, 277-291.
- (95) Valden, M.; Lai, X.; Goodman, D. W. *Science* **1998**, *281*, 1647-1650.
- (96) Bai, L.; Wang, X.; Chen, Q.; Ye, Y.; Zheng, H.; Guo, J.; Yin, Y.; Gao, C. *Angew. Chem. Int. Ed.* **2016**, 15656-15661.
- (97) Li, G.; Jiang, D. E.; Kumar, S.; Chen, Y. X.; Jin, R. C. *ACS Catal.* **2014**, *4*, 2463-2469.
- (98) Zhu, Y.; Wu, Z.; Gayathri, C.; Qian, H.; Gil, R. R.; Jin, R. *J. Catal.* **2010**, *271*, 155-160.
- (99) Zhu, Y.; Qian, H.; Zhu, M.; Jin, R. *Adv. Mater.* **2010**, *22*, 1915-1920.
- (100) Ohyama, J.; Esaki, A.; Yamamoto, Y.; Arai, S.; Satsuma, A. *RSC Adv.* **2013**, *3*, 1033-1036.
- (101) Liu, W. J.; Sun, D. R.; Fu, J. L.; Yuan, R. S.; Li, Z. H. *RSC Adv.* **2014**, *4*, 11003-11011.
- (102) E. Bailie, J.; J. Hutchings, G. *Chem. Commun.* **1999**, 2151-2152.
- (103) Cardenas-Lizana, F.; Gomez-Quero, S.; Perret, N.; Keane, M. A. *Catal. Sci. Technol.* **2011**, *1*, 652-661.
- (104) Hashmi, A. S. K.; Hutchings, G. J. *Angew. Chem. Int. Ed.* **2006**, *45*, 7896-7936.
- (105) Delannoy, L.; Weiher, N.; Tsapatsaris, N.; Beesley, A. M.; Nchari, L.; Schroeder, S. L. M.; Louis, C. *Top. Catal.* **2007**, *44*, 263-273.
- (106) Jupille, J.; Thornton, G. *Defects at Oxide Surfaces*; Springer International Publishing, 2015.
- (107) Juarez, R.; Parker, S. F.; Concepcion, P.; Corma, A.; Garcia, H. *Chem. Sci.* **2010**, *1*, 731-738.
- (108) Wang, L.; Zhang, J.; Wang, H.; Shao, Y.; Liu, X. H.; Wang, Y. Q.; Lewis, J. P.; Xiao, F. S. *ACS Catal.* **2016**, *6*, 4110-4116.
- (109) Yang, X.; Kattel, S.; Senanayake, S. D.; Boscoboinik, J. A.; Nie, X.; Graciani, J.; Rodriguez, J. A.; Liu, P.; Stacchiola, D. J.; Chen, J. G. *J. Am. Chem. Soc.* **2015**, *137*, 10104-10107.
- (110) Hirunsit, P.; Shimizu, K.; Fukuda, R.; Namuangruk, S.; Morikawa, Y.; Ehara, M. *J. Phys. Chem. C* **2014**, *118*, 7996-8006.
- (111) Hartfelder, U.; Kartusch, C.; Makosch, M.; Rovezzi, M.; Sa, J.; van Bokhoven, J. A. *Catal. Sci. Technol.* **2013**, *3*, 454-461.
- (112) Shimizu, K.; Kon, K.; Shimura, K.; Hakim, S. S. M. A. *J. Catal.* **2013**, *300*, 242-250.
- (113) García-Melchor, M.; López, N. *J. Phys. Chem. C* **2014**, *118*, 10921-10926.
- (114) Joubert, J.; Salameh, A.; Krakoviack, V.; Delbecq, F.; Sautet, P.; Copéret, C.; Basset, J. M. *J. Phys. Chem. B* **2006**, *110*, 23944-23950.
- (115) Amenomiya, Y. *J. Catal.* **1971**, *22*, 109-122.
- (116) Larson, J. G.; Hall, W. K. *J. Phys. Chem.* **1965**, *69*, 3080-3089.
- (117) Dash, P.; Scott, R. W. *Chem. Commun.* **2009**, 812-814.
- (118) Corma, A.; Serna, P. *Nat. Protoc.* **2006**, *1*, 2590-2595.
- (119) Zhukhovitskiy, A. V.; MacLeod, M. J.; Johnson, J. A. *Chem. Rev.* **2015**, *115*, 11503-11532.
- (120) Crudden, C. M.; Horton, J. H.; Ebralidze, I. I.; Zenkina, O. V.; McLean, A. B.; Drevniok, B.; She, Z.; Kraatz, H.-B.; Mosey, N. J.; Seki, T.; Keske, E. C.; Leake, J. D.; Rousina-Webb, A.; Wu, G. *Nat. Chem.* **2014**, *6*, 409-414.
- (121) Filonenko, G. A.; Vrijburg, W. L.; Hensen, E. J. M.; Pidko, E. A. *J. Catal.* **2016**, *343*, 97-105.
- (122) Tao, L.; Zhang, Q.; Li, S. S.; Liu, X.; Liu, Y. M.; Cao, Y. *Adv. Synth. Catal.* **2015**, *357*, 753-760.
- (123) Lu, G.; Zhang, P.; Sun, D.; Wang, L.; Zhou, K.; Wang, Z.-X.; Guo, G.-C. *Chem. Sci.* **2014**, *5*, 1082-1090.
- (124) Ren, D.; He, L.; Yu, L.; Ding, R. S.; Liu, Y. M.; Cao, Y.; He, H. Y.; Fan, K. N. *J. Am. Chem. Soc.* **2012**, *134*, 17592-17598.

- (125) Stephan, D. W.; Erker, G. *Angew. Chem. Int Ed.* **2015**, *54*, 6400-6441.
- (126) Mavlyankariev, S. A.; Ahlers, S. J.; Kondratenko, V. A.; Linke, D.; Kondratenko, E. V. *ACS Catal.* **2016**, *6*, 3317-3325.
- (127) Souza, L. C. M.; Santos, T. A.; Do Prado, C. R. A.; Lima, B. A. V.; Correa, R. S.; Batista, A. A.; Otubo, L.; Ellena, J.; Ueno, L. T.; Dinelli, L. R.; Bogado, A. L. *RSC Adv.* **2016**, *6*, 53130-53139.
- (128) Escalle, A.; Mora, G.; Gagosz, F.; Mézailles, N.; Le Goff, X. F.; Jean, Y.; Le Floch, P. *Inorg. Chem.* **2009**, *48*, 8415-8422.
- (129) Ito, H.; Saito, T.; Miyahara, T.; Zhong, C.; Sawamura, M. *Organometallics* **2009**, *28*, 4829-4840.
- (130) Liu, Z. P.; Wang, C. M.; Fan, K. N. *Angew. Chem. Int. Ed.* **2006**, *45*, 6865-6868.
- (131) Chen, J. Q.; Halin, S. J. A.; Perez Ferrandez, D. M.; Schouten, J. C.; Nijhuis, T. A. *J. Catal.* **2012**, *285*, 324-327.
- (132) Qi, C.; Huang, J.; Bao, S.; Su, H.; Akita, T.; Haruta, M. *J. Catal.* **2011**, *281*, 12-20.
- (133) Saavedra, J.; Whittaker, T.; Chen, Z.; Pursell, C. J.; Rioux, R. M.; Chandler, B. D. *Nat. Chem.* **2016**, *8*, 584-589.
- (134) Bu, W.; Zhao, L.; Zhang, Z.; Zhang, X.; Gao, J.; Xu, C. *Appl. Surf. Sci.* **2014**, *289*, 6-13.
- (135) Han, L.; Park, S.-W.; Park, D.-W. *Energy & Environmental Science* **2009**, *2*, 1286-1292.
- (136) Luska, K. L.; Julis, J.; Stavitski, E.; Zakharov, D. N.; Adams, A.; Leitner, W. *Chem. Sci.* **2014**, *5*, 4895-4905.
- (137) Umpierre, A. P.; de Jesús, E.; Dupont, J. *ChemCatChem* **2011**, *3*, 1413-1418.